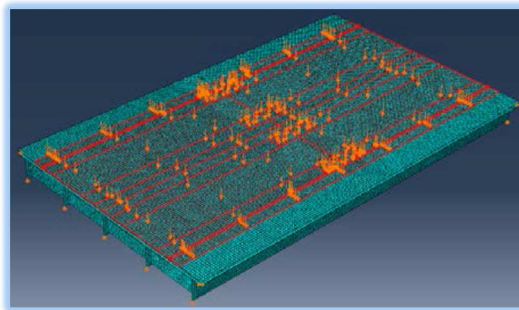**MaineDOT**

Transportation Research Division

Technical Report 20-01

Investigation of Behavior of Skewed and Un-Skewed Reinforced Concrete T-Beam Bridges and Load Rating Improvement through Proxy Finite Element Analysis

Technical Report Documentation Page

1. Report No. ME 20-01	2.	3. Recipient's Accession No.	
4. Title and Subtitle Investigation of Behavior of Skewed and Un-Skewed Reinforced Concrete T-Beam Bridges and Load Rating Improvement through Proxy Finite Element Analysis		5. Report Date December 2019	
		6.	
7. Author(s) Andrew Schanck, E.I., Graduate Researcher Bill Davids, Ph.D., P.E.		8. Performing Organization Report No.	
9. Performing Organization Name and Address University of Maine		10. Project/Task/Work Unit No. Project 23833.00	
		11. Contract © or Grant (G) No.	
12. Sponsoring Organization Name and Address Maine Department of Transportation 16 State House Station Augusta, Maine 04333		13. Type of Report and Period Covered	
		14. Sponsoring Agency Code	
15. Supplementary Notes			

16. Abstract (Limit 200 words)

Maine's bridge inventory includes a significant number of reinforced concrete T-beam bridges, both with and without skew. Many of these bridges were built in the first half of the 20th century for design loadings much lower than those considered today, causing a significant number of them to have low flexural rating factors. Despite this, these bridges continue to carry modern levels of loading with little to no apparent distress. This observation has resulted in new efforts to better understand the behavior of these bridges and to develop new methods of analysis which more accurately reflect their true capacities.

In the summers of 2017 and 2018, ten reinforced concrete T-beam bridges were non-destructively live-load tested to update their rating factors and to observe their load-strain responses. Five bridges were un-skewed and five were skewed between 15° and 35° relative to a perpendicular alignment. This selection of tested bridges allowed their responses to loading to be compared with the aim of identifying differences in behavior arising from the presence of skew. The understanding of these differences was also enhanced through the construction, calibration, and analysis of detailed, linear finite element models of the tested bridges.

The ten bridges that had been live-load tested were also load-rated through Proxy FEA to give a more accurate picture of their behavior at capacity. Each of these bridges' flexural rating factors were able to be significantly improved relative to their AASHTO calculated ratings, and nine of the ten were improved relative to their ratings updated through live-load testing. It is demonstrated that these ratings are optimistic, yet also realistic considering the technique's reliance on well-established mechanics and conservative assumptions. The possible future development of this technique as a general load rating tool for older structures is discussed.

17. Document Analysis/Descriptors Reinforced concrete T-beam bridges, load rating, live load testing	18. Availability Statement		
19. Security Class (this report)	20. Security Class (this page)	21. No. of Pages 54	22. Price

Investigation of Behavior of Skewed and Un-Skewed Reinforced Concrete T-Beam Bridges and Load Rating Improvement through Proxy Finite Element Analysis

Prepared for:
Dale Peabody P.E.
Director Transportation Research
Maine Dept. of Transportation
16 State House Station
Augusta ME 04333-0016
University of Maine's Advanced Structures and Composites Center
Report Number: 20-20-1613

2019-12-20-Rev00

Prepared by:
Andrew Schanck MSc, EI
Graduate Researcher

Reviewed by:
William G. Davids, PhD, PE
John C. Bridge Professor and Chair
Dept. of Civil and Environmental
Engineering

Investigation of Behavior of Skewed and Un-Skewed Reinforced Concrete T-Beam Bridges and Load Rating Improvement Through Proxy Finite Element Analysis

UMaine Composites Center Report 20-20-1613

Document Log

Name/ Organization	Date	Version	Action
Andrew Schanck, Author William Davids, Reviewer	2019-12-20	Rev00	Initial release to MaineDOT.

Table of Contents

Investigation of Behavior of Skewed and Un-Skewed Reinforced Concrete T-Beam Bridges and Load Rating Improvement Through Proxy Finite Element Analysis

UMaine Composites Center Report 20-20-1613

Index of Figures

Investigation of Behavior of Skewed and Un-Skewed Reinforced Concrete T-Beam Bridges and Load Rating Improvement Through Proxy Finite Element Analysis

UMaine Composites Center Report 20-20-1613

Index of Tables

Investigation of Behavior of Skewed and Un-Skewed Reinforced Concrete T-Beam Bridges and Load Rating Improvement Through Proxy Finite Element Analysis

UMaine Composites Center Report 20-20-1613

Executive Summary

Maine's bridge inventory includes a significant number of reinforced concrete T-beam bridges, both with and without skew. Many of these bridges were built in the first half of the 20th century for design loadings much lower than those considered today, causing a significant number of them to have low flexural rating factors. Despite this, these bridges continue to carry modern levels of loading with little to no apparent distress. This observation has resulted in new efforts to better understand the behavior of these bridges and to develop new methods of analysis which more accurately reflect their true capacities.

In the summers of 2017 and 2018, ten reinforced concrete T-beam bridges were non-destructively live-load tested to update their rating factors and to observe their load-strain responses. Five bridges were un-skewed and five were skewed between 15° and 35° relative to a perpendicular alignment. This selection of tested bridges allowed their responses to loading to be compared with the aim of identifying differences in behavior arising from the presence of skew. The understanding of these differences was also enhanced through the construction, calibration, and analysis of detailed, linear finite element models of the tested bridges. Two major differences in behavior between the skewed and un-skewed bridges were identified from comparative analysis of recorded strain response:

- For the same level of loading placed at different transverse positions, skewed bridges tended to distribute much more load to girders closer to the load than un-skewed bridges, which tended to distribute load more evenly.

- Four of the five skewed bridges displayed significant degrees of girder end fixity (as indicated by large measured bottom-fiber negative strains near the girder ends) whereas none of the un-skewed bridges displayed this behavior.

Results of the finite element analyses, along with additional investigation of data collected during testing led to the identification of plausible reasons for the differences in behavior. These are, respectively:

- Loads placed to one side of a skewed bridge are closer to the support at the obtuse corner than loads shifted to the side of an equivalent un-skewed bridge. This proximity tends to dominate the load-path, leading to increased levels of load being distributed through the exterior girder to the support at the obtuse corner.

- When unrestricted, skewed bridges tend to undergo warping deflections under vertical load which are not present in un-skewed bridges. This deflection could allow the ingress of large amounts of granular fill and debris from the road surface, which partially restricts the rotation of the girders and induces negative strain in the bottom fiber near the girder ends.

Investigation of Behavior of Skewed and Un-Skewed Reinforced Concrete T-Beam Bridges and Load Rating Improvement Through Proxy Finite Element Analysis

UMaine Composites Center Report 20-20-1613

To more accurately assess the live-load capacity of older T-beam bridges, a novel, nonlinear finite element technique, Proxy Finite Element Analysis (PFEA), was developed. This technique seeks to represent the complex material and system behavior of a bridge using proxy girder models whose flexural behavior closely matches that of an actual girder, but whose constitutive properties and geometry are straightforward to implement within commercial finite element software. The models utilize the full, nonlinear moment-curvature relationship of the individual girders and treat the bridge as a structural system rather than a collection of separate members. This allows full bridge models to simulate redistribution of load from heavily loaded girders to more lightly loaded girders, and allows the heavily loaded girders to undergo a realistic level of ductile, inelastic deformation before capacity is reached. This ductility and load redistribution cannot be captured by linearly elastic models.

The ten bridges that had been live-load tested were also load-rated through PFEA to give a more accurate picture of their behavior at capacity. Each of these bridges' flexural rating factors were able to be significantly improved relative to their AASHTO calculated ratings, and nine of the ten were improved relative to their ratings updated through live-load testing. It is demonstrated that these ratings are optimistic, yet also realistic considering the technique's reliance on well-established mechanics and conservative assumptions. The possible future development of this technique as a general load rating tool for older structures is discussed.

Investigation of Behavior of Skewed and Un-Skewed Reinforced Concrete T-Beam Bridges and Load Rating Improvement Through Proxy Finite Element Analysis

UMaine Composites Center Report 20-20-1613

1   Introduction

Reinforced Concrete (RC) T-beam bridges make up approximately 11% of Maine's bridge inventory. Due to their ages and the low loads for which they were designed, traditional engineering analysis specified by AASHTO (2011, 2012) results in many of these bridges being assigned operating flexural rating factors (*RFs*) less than 1.0. This designation indicates a need for remedial actions, which could include posting, repair, or replacement. However, most of these structures – including those for which traditional analysis indicates deficiencies – routinely carry modern loading without distress. For this reason, efforts have been made to more accurately characterize these structures' responses to load through live-load testing, specification of behavior, and advanced numerical analysis.

In this study, a sample of Maine's RC T-beam population was tested and analyzed in order to better understand its behavior and more accurately characterize the expected ultimate capacity of T-beam bridges. Specifically, two subsamples with un-skewed and skewed alignments (with other geometric parameters kept as consistent as possible) were selected to identify the effects skewness has on bridge behavior. These bridges were also used as test-beds for improved load-rating procedures based on live-load testing and nonlinear finite element (FE) analysis.

1.1   Scope of Tasks

The entirety of this project consisted of three tasks, two of which (Tasks 2 and 3) are discussed in detail in this report. Task 1 involved instrumentation and live-load testing of five skewed, RC T-Beam bridges in the state of Maine, recording strain data and using those data to update the bridges' *RFs* based on allowances by AASHTO (2011). Details of this task can be found in Schanck and Davids (2018b). Task 2 sought to identify differences in behavior between similar skewed and un-skewed RC T-beam bridges by analyzing recorded live-load strain response data, and enhancing the understanding of these differences using the results of linear, 3-D FE models. Finally, Task 3 sought to improve capacity rating of RC T-beam bridges using FE analysis.

1.2   Description of Bridges

A brief summary of the 10 tested bridges is given here, and much greater detail can be found in Schanck and Davids (2018a, 2018b).

1.2.1   Un-Skewed Bridges

Five un-skewed, RC T-beam bridges in Maine were live-load tested in the summer of 2017. These were each built between 1936 and 1950, with span lengths ranging between 27 and 43 ft. Prior to live-load testing, these bridges' operating flexural *RFs* ranged between 0.24 and 1.12, but based on the results of testing were increased to between 0.30 and 1.95, bringing the controlling *RF* of four of the five bridges above 1.0.

Investigation of Behavior of Skewed and Un-Skewed Reinforced Concrete T-Beam Bridges and Load Rating Improvement Through Proxy Finite Element Analysis

UMaine Composites Center Report 20-20-1613

1.2.2 Skewed Bridges

Five skewed, RC T-beam bridges in Maine were live-load tested in the summer of 2018. These were each built between 1931 and 1952, with span lengths ranging between 34 and 50 ft. Angles of skew ranged between 15° and 35°. Prior to live-load testing, these bridges' operating flexural *RFs* ranged between 0.69 and 1.09, but based on the results of testing were increased to between 0.84 and 1.35, bringing the controlling *RF* of three of the five bridges above 1.0.

2   Data Processing and Linear Finite Element Model Generation

In order to compare the behavior of un-skewed and skewed RC T-beam bridges under live-load, diagnostic live-load field tests were conducted with bridge load response captured through strains. These data were then processed to facilitate analysis and filter out the effects of imperfect sensors and spurious data. Finally, detailed, linear 3-D FE models were constructed and calibrated to adequately match test results so as to enhance understanding of the results of data analysis.

2.1   Live-Load Test Procedure

The procedure for performing diagnostic live-load tests has been well documented in previous reports (for instance Schanck and Davids (2018a, 2018b)) and recent journal papers (Albraheemi et al. 2019; Schanck and Davids 2020) and so will not be explained here in great depth. However, a brief description will be given for reference. When bridges are tested, they are first instrumented at specific locations with Bridge Diagnostics Incorporated (BDI) integrated strain transducers, which are attached at specific points to capture certain effects. For the bridges tested, transducers were adhered to each girder at midspan at three points along its height so as to measure both the maximum strain in each girder and the distribution of strains through its depth. In addition, transducers were adhered to girders' ends at their bottoms to monitor unintended support restraint, as indicated by recorded negative strains.

After bridges had been instrumented, live loads equal to ~80% of two lanes of HL-93 live load with impact were applied and girder strain responses were measured. Load was applied using overloaded dump trucks which were systematically driven onto the bridge and parked at predetermined locations. These trucks' individual wheel weights, axle spacings, and tire contact areas had been measured beforehand to determine the total load applied, and the trucks' positions on the bridge during each test were measured to calculate the actual applied moment. These measurements were also used to accurately apply load to the subsequent FE models. For each test, either two trucks or four trucks were placed on the bridge, and arranged to apply maximum levels of moment to specific locations.

Investigation of Behavior of Skewed and Un-Skewed Reinforced Concrete T-Beam Bridges and Load Rating Improvement Through Proxy Finite Element Analysis

UMaine Composites Center Report 20-20-1613

2.2 Live-Load Test Data Extraction and Rectification

After all data had been extracted they were rectified to make them useful for analysis. Initially, all data were rectified to correct for the BDI transducers' tendency to zero-drift over the course of a test. This was done for the data recorded by each transducer by finding the slope of the line between the first and last recorded data points (both of which were known to be recorded at points of zero live-load strain) and subsequently offsetting each strain data point proportional to the elapsed time and the slope of the zero-drift line. In this way all data could be referenced to a common zero.

With initial rectification completed, specific subsets of the recorded data from each test could be extracted for analysis. For these analyses, it was most important to capture the bridges' behaviors under the maximum static loading condition applied. Therefore, the data recorded from the most heavily loaded girder in each test was examined, and a point occurring during the load plateau following application of the last truck per test was selected as the reference point. This ensured that the bridge's maximum response to the particular loading was captured, while also eliminating any dynamic effects. The elapsed time at which the reference point was recorded was noted and used as a reference time at which the data points from all other transducers were extracted. These strains were then arranged in tabular form for initial analysis and further rectification.

Although care was taken to measure strains accurately, it is inevitable during field-testing that some recorded data be unreliable for a number of reasons. This is usually manifested as recorded strains which are unreasonably low relative to other strains recorded at the same section, thus grossly violating the assumption of linear strain variation through the girder depth. For data recorded at a bridge's midspan, correcting unreliable data was straightforward (assuming that only one transducer's data was unreliable) as three sensors are used across the depth of the section. In such cases, the depth of the girder's neutral axis was estimated using the readings from the remaining two transducers and, assuming linear strain distribution, the corrected reading calculated based on the height of the third transducer within the section. Unreliable strains at girder ends were much less straightforward to identify and rectify. Because, at most, only two sensors were used at a girder's end, and the assumption of linear strain distribution could not be easily used to identify unreliable data. Thus, data were only deemed unreliable at the girder end if the particular transducer from which they were collected did not change its reading, regardless of the actual loading. When that was the case, these data were discarded, but this was much rarer an occurrence than the occurrence of unreliable data at midspan.

2.3 Linear Finite Element Models

To enhance the understanding of bridge behavior observed from live-load testing, linear, 3-D FE models were generated of each bridge which simulated the conditions of each test. These models were highly detailed, incorporating many of the features present in the real bridges that may affect live-load response, including discrete reinforcing steel, composite curbs and wearing surfaces, and

Investigation of Behavior of Skewed and Un-Skewed Reinforced Concrete T-Beam Bridges and Load Rating Improvement Through Proxy Finite Element Analysis

UMaine Composites Center Report 20-20-1613

railings. These models were first built with their respective bridge's nominal geometric and material parameters, and then were systematically calibrated such that they adequately predicted the real bridges' responses to loading.

Modeling and analysis were performed using the commercial FE software ABAQUS (n.d.) due to the authors' familiarity with its use and its availability. The components of bridges made from concrete were modeled as isotropic, elastic continua using C3D20R 20-node, quadratic, brick elements with three degrees of freedom per node and reduced integration. These elements are able to yield accurate results with a coarser mesh than similar, linear continuum elements. In general, all concrete components which could reasonably contribute to a bridge's stiffness were modeled, including girders, deck, diaphragms, curbs, railings, and integral wearing surfaces. Reinforcing steel was explicitly modeled using isotropic, elastic beams using B32 quadratic, three-node beam elements with six degrees of freedom per node. All significant reinforcing bars, including girder longitudinal reinforcement, shear stirrups, and deck longitudinal and transverse reinforcement were modeled and kinematically tied to the concrete elements with embedment constraints. Typically, a model consisted of between 100,000 and 300,000 elements with 500,000 to 1,000,000 nodes and 1,000,000 to 3,000,000 degrees of freedom.

Load was applied to mimic the loading from trucks during testing while also accounting for the bridge's initial (dead-load) conditions. To simulate the effects of dead-loading and test live-loading independently, load was applied in two separate load steps with the effects of subsequent steps adding to the effects of previous steps. In the first load-step, gravitational dead-load was applied by assigning concrete elements a unit weight of $150 \, \text{lb/ft}^3$ and subjecting the entire model to a unit, downward gravitational field. The dead-load contributions from nonstructural components (for instance bituminous concrete wearing surfaces) were applied as pressure loads across the area of the superstructure over which they acted. In the live-load step, the test trucks' wheel weights were assumed to act uniformly over their tire contact areas and so were applied to the models as pressures. These pressure loads were distributed over areas corresponding to tire contact area, which were in turn located on the model in the locations measured during testing.

Boundary conditions were enforced to reasonably approximate the conditions of the real bridges. None of the bridges used true pin or roller type bearings. Instead, most were designed such that one end rested on the abutment with a layer of roofing felt between the girder and support, and the other rested on flat, bronze or steel expansion bearings. Additionally, the "pinned" side (the side without the expansion bearing) was often connected to the abutment with steel dowels embedded into both the foot of the girders and the top of the abutment. To emulate these conditions, rigid abutments were modeled upon which the bridge sat, with a frictionless contact condition enforced between them. This reasonably approximated the conditions of the actual bridge much better than would standard displacement boundary conditions. Where present, the dowel rods were explicitly

Investigation of Behavior of Skewed and Un-Skewed Reinforced Concrete T-Beam Bridges and Load Rating Improvement Through Proxy Finite Element Analysis

UMaine Composites Center Report 20-20-1613

modeled and embedded within both the superstructure and rigid abutment. This prevented instability due to transverse rigid body motion and rotation of the superstructure. Where dowel rods were not present, minimally restrictive displacement restraints were added to prevent rigid body displacements and rotations.

After all the models were constructed, they were calibrated such that their predicted strains agreed reasonably well with measured strains. Being that the models were perfectly linearly elastic, the models' responses could be reasonably controlled by altering their stiffnesses. This allowed calibration to be controlled by changing the elastic modulus of the concrete components of the models. In nearly all cases, the uncalibrated models predicted much larger strains than were measured in the field. This indicated that the models were not stiff enough and that increases to the concrete's elastic modulus in some or all of the concrete components would likely bring predictions better into line with measurements. This is justifiable given that previous studies of older bridges have shown the in-situ concrete compressive strengths of older bridges to be up to 220% greater than the design compressive strength (for instance Saraf (1998), Buckle et al. (1985)), and the concrete elastic modulus increases proportionally to the square root of its compressive strength. Models' concrete elastic moduli were systematically updated and simulations rerun until the moduli giving the best predictions were obtained for each bridge. These models could then be further examined to investigate observed behavioral differences between un-skewed and skewed bridges.

3   Comparisons of Skewed and Un-Skewed Bridge Behavior

The strains recorded during live-load were examined to determine any possible differences in the behavior of skewed RC T-beam bridges relative to similar un-skewed bridges. This required comparing the strains recorded within individual girders for similar tests of bridges, as well as comparing bridges' responses under different load-cases. These comparisons led to the identification of two specific differences in behavior between the types of bridges which will be explained in detail. The results of the linear FE models were then examined to better understand these behaviors and how skewness could cause them.

3.1   Load Distribution

A major point of interest when analyzing bridge structures is the way in which live-loads applied to the deck are distributed to individual girders. This has a significant impact on a bridge's *RF* – the primary measure of a bridge's live-load capacity and ability to carry modern loads – as it directly scales the demand placed on a particular girder. Therefore, gaining a better understanding of a bridge's live-load distribution characteristics is instrumental to understanding its overall behavior and live-load capacity. It should be noted that the load distribution properties discussed here are related to, but not the same as, distribution factors (*DFs*) as defined by AASHTO (2012)

Investigation of Behavior of Skewed and Un-Skewed Reinforced Concrete T-Beam Bridges and Load Rating Improvement Through Proxy Finite Element Analysis

UMaine Composites Center Report 20-20-1613

for design and analysis. *DFs* represent the maximum fraction of HL-93 live-load that can be attributed to any individual girder from all possible live loading scenarios. The fractions of live-load discussed here, called girder lane fractions (*GLFs*) describe the portion of live-load carried by a particular girder under one specific loading condition. However, due to the narrow, two-lane geometry of these simple-span bridges, and the fact that multiple load cases were applied in the field where trucks were shifted both longitudinally and transversely, the maximum *GLFs* derived from testing are expected to be very good approximations of the true girder *DFs*. Therefore, comparison between the *GLFs* and AASHTO *DFs* as presented later is appropriate.

GLFs, whether from live-load testing or FE analysis, are calculated by Equation 1, where $S_{i,j}$ is the uncracked section modulus of the ith or j^{th} girder, $\varepsilon_{i,j}$ is the measured or calculated strain in the ith or j^{th} girder, n is the total number of girders, and the 2 in the numerator indicates that two lanes of loading were applied.

$$GLF_i = \frac{2S_i\varepsilon_i}{\sum_{j=1}^{n} S_j\varepsilon_j} \qquad \text{Equation 1}$$

GLFs were calculated from a set of three tests in which the loading configuration was the same but the loads were placed in separate transverse positions (for instance, three tests in which four trucks were located longitudinally to produce maximum midspan moment but transversely close to the left curb, centerline, and right curb respectively). These were then examined to observe a particular bridges' sensitivity to transverse load position. To illustrate this, an example from an un-skewed bridge (Bridge 3307) and skewed bridge (Bridge 5489) are presented in Figures 1 and 2 respectively, with similar plots of seven of the remaining bridges presented in Figures 14-20 in Appendix A. (Note that because a set of three similar longitudinal but differing transverse loading tests were not performed for Bridge 3356, no plot was included.)

Investigation of Behavior of Skewed and Un-Skewed Reinforced Concrete T-Beam Bridges and Load Rating Improvement Through Proxy Finite Element Analysis

UMaine Composites Center Report 20-20-1613
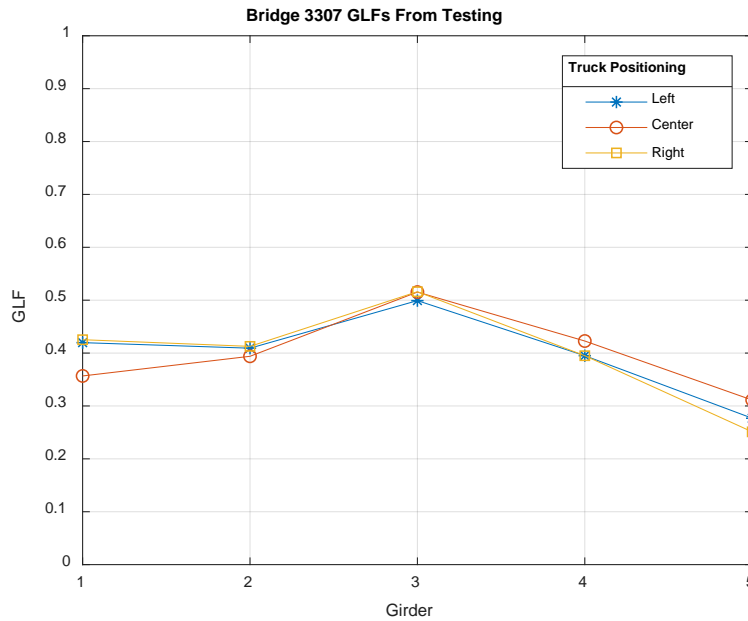
Figure 1: *GLFs* Calculated from Live-Load Testing – Bridge 3307 (Un-Skewed)
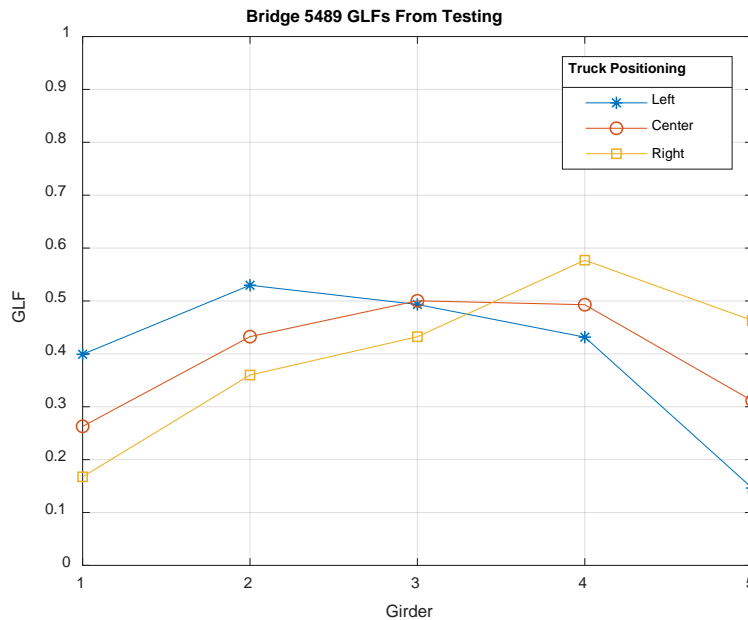

Figure 2: *GLFs* Calculated from Live-Load Testing – Bridge 5489 (Skewed)

GLFs calculated for these sets of tests appear to indicate a correlation between skewness and a bridge's sensitivity to load position. As seen from Figure 1, movement of trucks transversely from the left side of Bridge 3307 to the center and then to the right side had very small effects on

Investigation of Behavior of Skewed and Un-Skewed Reinforced Concrete T-Beam Bridges and Load Rating Improvement Through Proxy Finite Element Analysis

UMaine Composites Center Report 20-20-1613

individual girders' *GLF*. The opposite is true for Bridge 5489 as seen in Figure 2, where transverse movement of loads resulted in large changes of *GLF*, especially for exterior girders. Table 1 presents the difference between maximum and minimum calculated *GLF* for each girder of each bridge from the three, 4-truck load cases.

Table 1: Maximum Change in *GLF* from Live-Load Testing

Bridge	Skew Angle (deg)	Change in *GLF*				
		Girder 1	Girder 2	Girder 3	Girder 4	Girder5
2130	0	0.018	0.054	0.039	0.102	-
3307	0	0.069	0.019	0.017	0.028	0.060
3776	0	0.118	0.098	0.009	0.071	0.142
5432	0	0.090	0.074	0.029	0.046	0.088
2390	30	0.110	0.088	0.039	0.070	0.162
2879	30	0.143	0.084	0.052	0.175	-
3848	30	0.157	0.098	0.051	0.084	0.119
5109	35	0.282	0.195	0.063	0.291	0.130
5489	15	0.232	0.170	0.068	0.146	0.317

As can immediately be seen, the skewed bridges tended to display much larger changes in GLF than un-skewed bridges under similar load configurations. Additionally, the largest changes in *GLF* tended to occur in exterior girders, while smaller changes tended to occur in the central girders. The large changes in load distribution of skewed bridges as compared with un-skewed bridges is likely due in part to differences in available load-path. In un-skewed bridges a load at the center (longitudinally and transversely) of the deck is equidistant to each of the four corners of the bridge and so, all else being equal, load will be attracted equally by both ends longitudinally and at each end, load would be attracted to supports symmetrically about the transverse centerline. Conversely, in a skewed bridge the same load is closer to the obtuse corners than to the acute corners, and so the load path will tend to favor the obtuse side much more heavily.

To investigate whether differences in load-path could explain the differences in load distribution between un-skewed and skewed bridges, the results of the linear FE models were examined, paying attention to the live-load reactions at each end of each girder under load from the three tests with differing transverse truck placement. This revealed the percentage of load attracted to each end of the bridge as well as the amount of load attracted by each girder for the same levels of loading placed in three transverse positions across the deck. Figures 3 and 4 show the reaction forces calculated for each support of Bridge 5432 (an un-skewed bridge) as fractions of the total load attracted by each end, and Figures 5 and 6 show the reaction forces calculated for each support of Bridge 3848 (a skewed bridge), also as fractions of the load attracted by each end. Similar plots for the other bridges (again with the exception of Bridge 3356) are presented in Figures 21-34 in Appendix A.

Investigation of Behavior of Skewed and Un-Skewed Reinforced Concrete T-Beam Bridges and Load Rating Improvement Through Proxy Finite Element Analysis

UMaine Composites Center Report 20-20-1613

Figure 3: Fractions of Reaction Force Attracted to Each Support at Side 1 – Bridge 5432 (Un-Skewed)

Figure 4: Fractions of Reaction Force Attracted to Each Support at Side 2 – Bridge 5432 (Un-Skewed)

Investigation of Behavior of Skewed and Un-Skewed Reinforced Concrete T-Beam Bridges and Load Rating Improvement Through Proxy Finite Element Analysis
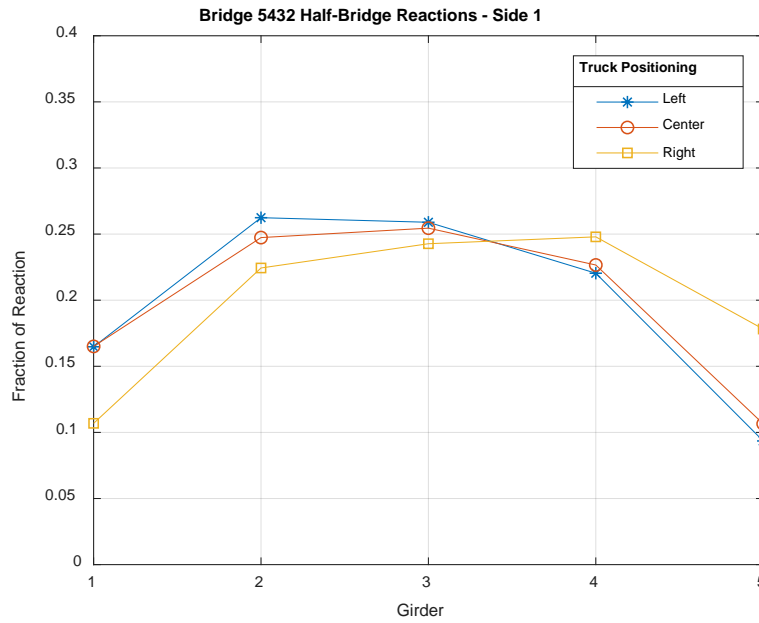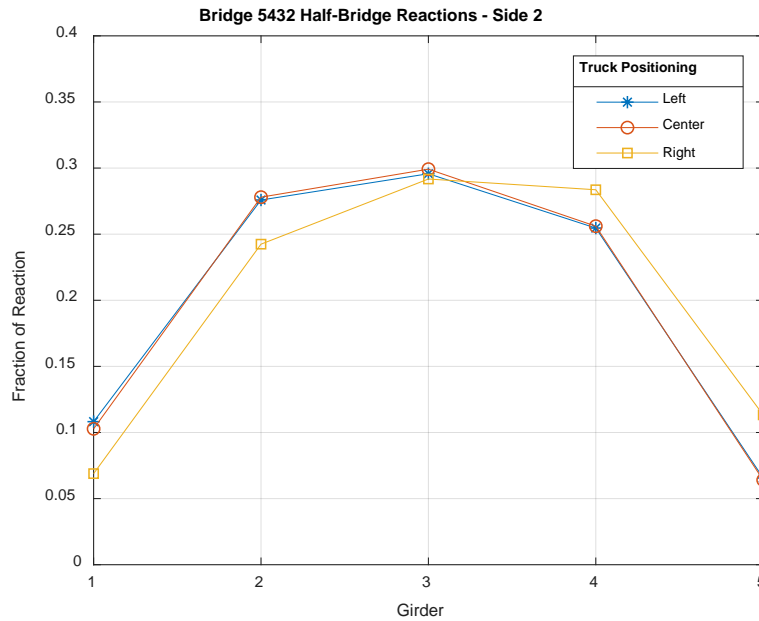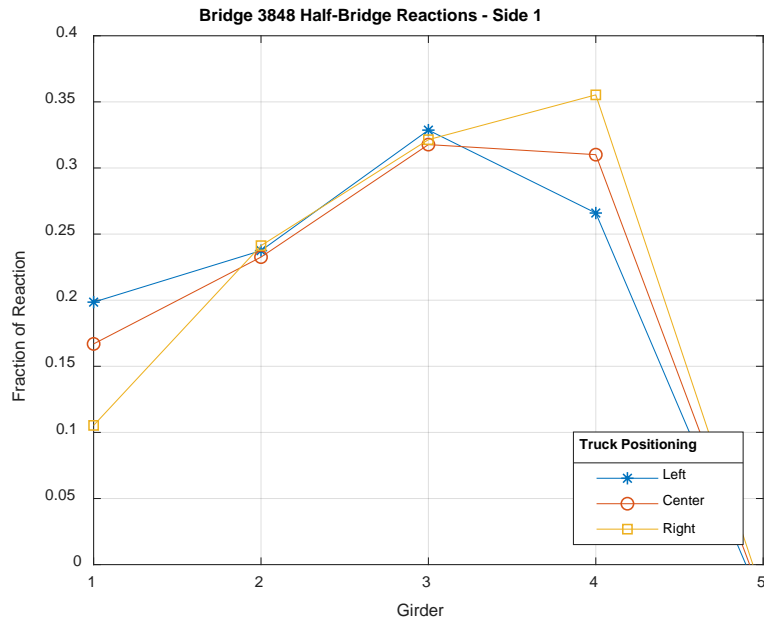
UMaine Composites Center Report 20-20-1613

Figure 5: Fractions of Reaction Force Attracted to Each Support at Side 1 – Bridge 3848 (Skewed)

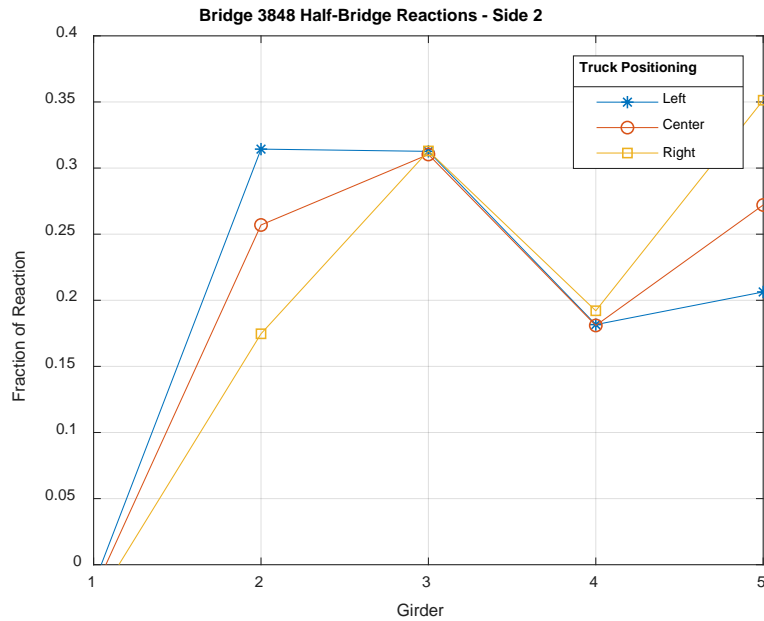Figure 6: Fractions of Reaction Force Attracted to Each Support at Side 2 – Bridge 3848 (Skewed)

Investigation of Behavior of Skewed and Un-Skewed Reinforced Concrete T-Beam Bridges and Load Rating Improvement Through Proxy Finite Element Analysis

UMaine Composites Center Report 20-20-1613

Figures 3 and 4 show that the support reactions are roughly consistent with those expected for the un-skewed bridge: reactions are fairly symmetric about the transverse centerline with a small amount of offset due to the different weights of the trucks used and their transverse positions. On the other hand, Figures 5 and 6 show very different behavior. For each end of Bridge 3848, one transverse side attracts significantly more load than the other. The preferred side corresponds with the side with the obtuse corner. It should also be noted that the reactions at the acute corners are negative for live-loading, meaning that the loading caused a lessening of the reaction due to dead-load. This behavior is consistent with the assumption that the bridge's load-path is significantly affected by the load's proximity to the obtuse corner. This could explain why the skewed bridges' load distributions appear to be more sensitive to transverse load placement as loads closer to one side of the bridge will be much more heavily attracted to the obtuse corner.

3.2 *Comparison with AASHTO Live Load Distribution Factors*

As noted before, the *GLF*s inferred from the results of live-load testing and calculated based on results of FE analyses are related to AASHTO *DFs* in that they describe the distribution of loads to individual girders, but are valid only for the loading configuration from which they were inferred or calculated. However, the bridges live-load tested were relatively narrow, allowing the three transverse loading positions considered to capture the effects of most possible transverse loading conditions. This allows flexural *DF*s to be reasonably approximated as the maximum *GLF*s from any interior and exterior girder inferred or calculated for each bridge. Table 2 presents the AASHTO calculated *DF*s and *DF*s approximated from testing and FEA for each bridge (with the exception of Bridge 3356).

Table 2: Comparison of AASHTO *DF*s and Approximate *DF*s

Bridge	Skew (°)	AASHTO *DF*		Max *GLF* from Testing		Max *GLF* from FEA	
		Interior	*Exterior*	*Interior*	*Exterior*	*Interior*	*Exterior*
2130	0	0.707	0.485	0.870	0.351	0.808	0.315
3307	0	0.600	0.432	0.516	0.425	0.506	0.358
3776	0	0.635	0.396	0.579	0.439	0.471	0.484
5432	0	0.680	0.473	0.522	0.382	0.474	0.387
2390	30	0.635	0.428	0.629	0.325	0.560	0.411
2879	30	0.701	0.498	0.660	0.543	0.642	0.499
3848	30	0.611	0.431	0.528	0.440	0.526	0.460
3848	35	0.686	0.506	0.646	0.440	0.531	0.567
5489	15	0.685	0.483	0.577	0.463	0.491	0.495

Investigation of Behavior of Skewed and Un-Skewed Reinforced Concrete T-Beam Bridges and Load Rating Improvement Through Proxy Finite Element Analysis

UMaine Composites Center Report 20-20-1613

As Table 2 shows, nearly all of the AASHTO interior girder *DF*s were conservative, whereas more than half the AASHTO exterior *DF*s were unconservative relative to the approximate *DF*s from testing and/or FEA. For the skewed bridges, two exterior AASHTO *DF*s were unconservative compared with field testing *GLF*s, and only one exterior AASHTO *DF* was unconservative compared with field test *GLF*s for the un-skewed bridges. To examine whether a trend exists, the percent error in approximate *DF*s relative to AASHTO *DF*s were calculated and are plotted in Figure 7. In these plots, a negative percent error represents a conservative estimation of *DF* by AASHTO and a positive percent error represents an unconservative estimation. These plots do not show a clear trend in *DF* prediction accuracy with increasing angle of skew, suggesting that such a correlation may not exist.
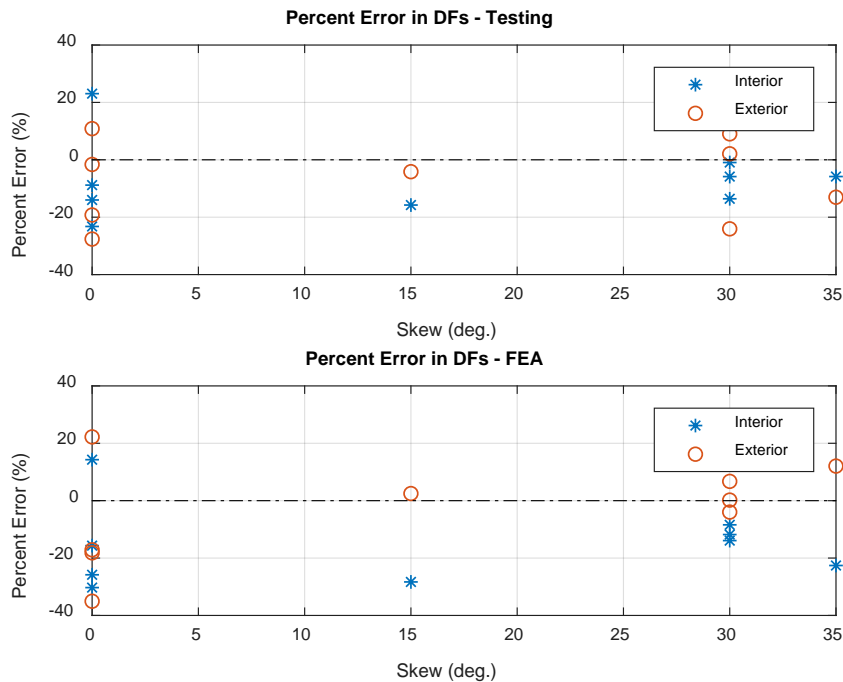
Figure 7: Percent Error in Approximate *DF*s Relative to AASHTO *DF*s

3.3 Support Fixity

Support conditions play a vital role in a bridge's behavior – especially as pertains to the level of strain to which a girder is subjected (and thus the resulting moment). Although many bridges (including all of the bridges investigated as part of this study) are designed to behave as simply supported, actual conditions can result in a certain amount of bearing fixity that affects their behavior. This fixity can be caused by numerous factors, and can often be detected through live-load testing as negative strains recorded close to the girder supports.

Investigation of Behavior of Skewed and Un-Skewed Reinforced Concrete T-Beam Bridges and Load Rating Improvement Through Proxy Finite Element Analysis

UMaine Composites Center Report 20-20-1613

Along with the transducers used to detect strains at midspan, some girders of each bridge were instrumented at their ends to monitor fixity. At a minimum, for the instrumented girders, one transducer was applied to the girder's bottom, although some also received a second transducer at the girder's mid-height. The bottom-mounted transducer recorded the maximum negative or positive strain response at the girder's end depending on whether or not the girder experienced fixity, with large negative strains indicating a significant degree of unintended fixity. Table 2 presents the average, maximum, and minimum strains measured at the bottom of the ends of each girder for each bridge under 4-truck loading.

Table 3: Recorded Strains at Girder Ends from Live-Load Testing

Bridge	Skew Angle (deg.)	Average Strain (με)	Maximum Strain (με)	Minimum Strain (με)
2130	0	2.27	8.12	-2.88
3307	0	-0.43	7.62	-7.17
3356	0	6.21	13.73	-3.13
3776	0	6.39	13.14	1.55
5432	0	4.51	14.88	-5.13
2390	30	-15.50	1.24	-36.77
2879	30	7.89	11.04	5.69
3848	30	3.43	4.61	-22.82
5109	35	-10.33	4.61	-22.82
5489	15	-5.83	8.01	-24.19

The strains measured at the bottoms of girders near bearings were small relative to the maximum strains recorded at midspan, However, relative to each other the data recorded for skewed and un-skewed bridges show very different behavior. For all of the un-skewed bridges, the recorded strains were generally positive or at most only slightly negative indicating little to no fixity. The direct opposite is true for four of the skewed bridges. Relatively large negative strains were recorded from four of the five skewed bridges, indicating a high degree of support fixity, which likely reduced the strains recorded at midspan. Determining the sources of this fixity was important to determining its future reliability.

It was initially attempted to identify the sources of the skewed bridges' apparent fixity as part of the model calibration process. However, this strategy proved ineffective. The method used to reach better predictions of actual behavior – changing the elastic moduli of all or individual girders – improved the prediction of midspan strains, but could not produce negative girder end strains since it did not impact loading or support conditions. Adding fixity at the supports – either by enforcing additional boundary conditions or applying resistance in the form of linear spring elements to the girder ends – tended to moderately improve the prediction of strains at girder ends, but was severely detrimental to the prediction of midspan strains. Because of this, it was decided to ignore

Investigation of Behavior of Skewed and Un-Skewed Reinforced Concrete T-Beam Bridges and Load Rating Improvement Through Proxy Finite Element Analysis

UMaine Composites Center Report 20-20-1613

girder end strains in the calibration process in order to better predict midspan strains which were deemed more important to accurately predict.

With end fixity ignored, calibration of the skew bridge models commenced as described previously with the models analyzed under the load conditions from live-load testing. However, in reviewing the analysis results, a response was observed that had not been seen for the un-skewed bridges. Figure 8 presents images taken from the results of the analysis of the model of Bridge 3776 loaded by 4 trucks in the centered position from a top and bottom perspective (the model's deflected shape has been highly exaggerated for clarity). The colors on the model represent longitudinal displacement. This is contrasted with similar images from the results of Bridge 2390 under the same type of loading. As can be seen, Bridge 3776's longitudinal extension is fairly symmetric with the difference between the extension of the center girder and the exterior girders being around 0.004 in. This is in contrast with the results from similar loading of the model of Bridge 2390 in Figure 9, which shows asymmetrical displacement and a difference in extension between the exterior girders of around 0.013 in. This difference arises from torsional effects that are not present in the un-skewed bridges but are present in the results of the models of each of the skewed bridges.

$u_3 = 0.0072$ in

$u_3 = 0.003$ in
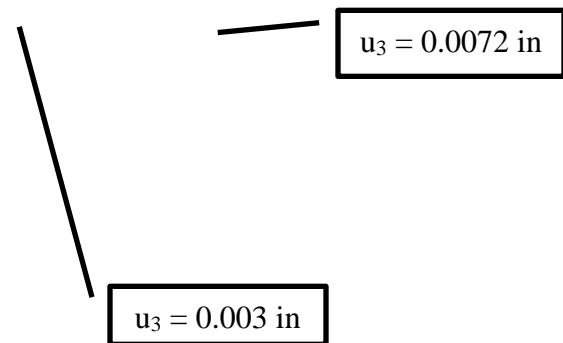
Figure 8: Calculated Longitudinal Displacement of Bridge 3776 (Left: Top view, Right: bottom view)

Investigation of Behavior of Skewed and Un-Skewed Reinforced Concrete T-Beam Bridges and Load Rating Improvement Through Proxy Finite Element Analysis

UMaine Composites Center Report 20-20-1613

$u_3 = 0.0075$ in

$u_3 = -0.006$ in
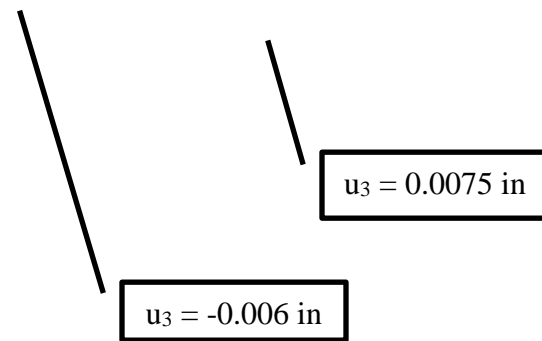
Figure 9: Calculated Longitudinal Displacement of Bridge 2390 (Left: Top view, Right: bottom view)

The identification of asymmetrical extension and twisting effects in skewed bridges does not lead directly to the cause of apparent girder end fixity. Rather, it points to the bridges' behaviors absent the cause of the observed fixity. However, consideration of the actual conditions of the bridges (as opposed to the models) allows for some speculation into a reasonable cause for the observed fixity. Each of these bridges include end diaphragms forming their backwalls. These backwalls are battered by a few degrees at the rear with granular fill behind. It is possible that due to their twisting motion, the skewed bridges have allowed more granular backfill to migrate underneath their backwalls, fouling their motion more than on the un-skewed bridges. This restriction of motion by debris, though difficult to identify and model, could lead to the apparent end fixity observed during testing.

As additional evidence of the hypothesis that skewed bridges' motion may be restricted by increased amounts of debris, photographs of the individual bridges taken during test set-up were examined, focusing on images that revealed the conditions of the girder ends and bearing areas. Figure 10 presents an image taken of one of the abutment and backwalls from Bridge 5432, an un-skewed bridge. As the image shows, the gap between the back-wall and the top of the abutment is fairly clean, with only a small amount of visible debris. This is contrasted with Figure 11, which presents a similar image taken from Bridge 5109. A significant amount of debris is visible in the gap between abutment and backwall, which could partially restrict the bridge's end rotation causing negative strains to develop.

Investigation of Behavior of Skewed and Un-Skewed Reinforced Concrete T-Beam Bridges and Load Rating Improvement Through Proxy Finite Element Analysis

UMaine Composites Center Report 20-20-1613
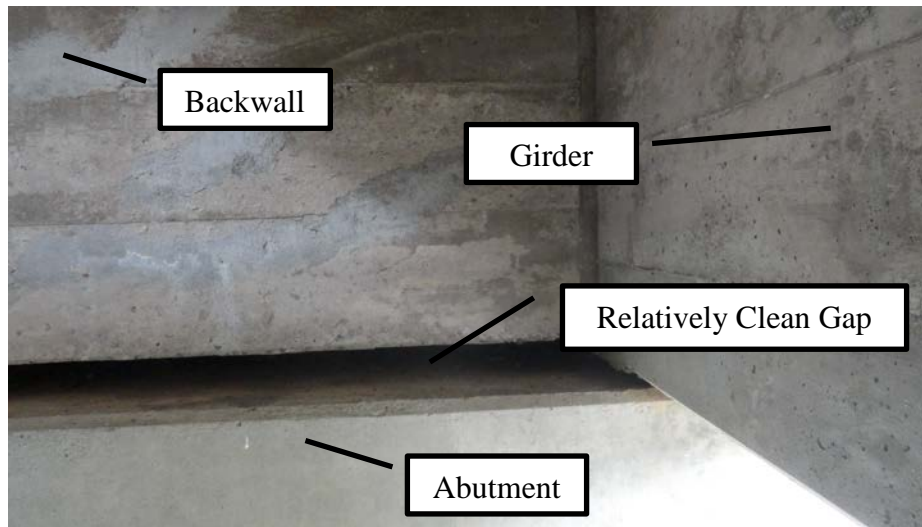
Figure 10: Condition of Gap Between Abutment and Backwall – Bridge 5432
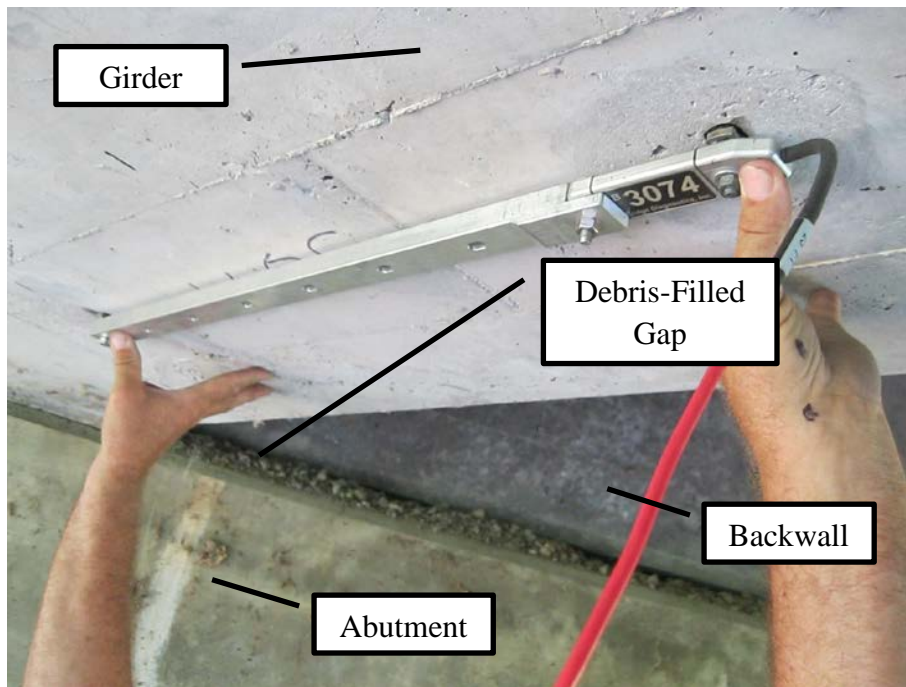
Figure 11: Condition of Gap Between Abutment and Backwall – Bridge 5109

Finally, this hypothesis of skewed bridges' tendency to collect bearing-fouling debris also explains why one of the five skewed bridges, Bridge 2879, did not appear to exhibit any significant girder end fixity. Bridge 2879 consists of four nominally identical, simple spans, with interior spans resting on piers and exterior spans resting on piers and abutments. The span that was live-load tested was an interior span, without any fill behind its backwalls. Without any fill available to

Investigation of Behavior of Skewed and Un-Skewed Reinforced Concrete T-Beam Bridges and Load Rating Improvement Through Proxy Finite Element Analysis

UMaine Composites Center Report 20-20-1613

restrict its motion, the tested span was able to deform much more freely, exhibiting end conditions that were much closer to simply supported than were observed for the other four skewed bridges. This may not have been the case had an exterior span been tested, as one of the ends would have had the potential to collect debris, restricting its motion.

4 Proxy Finite Element Analysis

The current method by which bridge live-load capacity is most often evaluated, using AASHTO code-based calculations to determine *RFs*, is analogous to the design of new bridges, using most of the same assumptions and empirical relations, and is thus subject to similar capacity requirements. However, for bridges designed under previous specifications, this method often predicts inadequate flexural capacity, leading to the perceived need for remedial actions, such as load posting, repair, or replacement. However, many of these bridges, such as most of the bridges live-load tested as part of this study, carry modern loads regularly with no apparent signs of distress despite their low *RFs*. This suggests that these bridges have higher capacities than are achievable under the assumptions from normal load rating, and that a method of load rating is required that overcomes the assumptions and limitations leading to this under-prediction of capacity.

To address the need for a new, more accurate method of load-rating older RC T-beam bridges, a novel, nonlinear FE analysis technique, dubbed proxy finite element analysis (PFEA), has been developed and is presently being further enhanced. This method overcomes the shortcomings of standard bridge flexural rating by accounting for the full, nonlinear constitutive properties of concrete and reinforcing steel and also by treating a bridge as a system of interrelated, interdependent components rather than a collection of individual, disparate members, yet also retains a number of conservative assumptions. Further, PFEA is much simpler to implement and more computationally tractable than a 3D nonlinear finite-element continuum analysis that accounts for concrete cracking and crushing. Using this method, the live-load tested bridges from this study were load-rated with promising, yet conservative results.

4.1 Proxy Finite Element Analysis Concept

The basic premise of PFEA is to capture a bridge girder's full longitudinal flexural behavior up to failure, including contributions from its geometry and possibly complicated material nonlinearity, and condense it into a single nonlinear relationship. This relationship is then imparted onto an equivalent section (a proxy section) whose geometry and constitutive behavior are straightforward to implement into commercial FE software. Proxy section girder models are then assembled into a 3D model of a full bridge which is loaded by both dead-load and increasing multiples of HL-93 live-load to complete bridge failure. The multiple of HL-93 live-load required to cause model failure directly represents the bridge's live-load capacity, from which its flexural *RF* may be calculated.

Investigation of Behavior of Skewed and Un-Skewed Reinforced Concrete T-Beam Bridges and Load Rating Improvement Through Proxy Finite Element Analysis

UMaine Composites Center Report 20-20-1613

4.2 Proxy Finite Element Analysis Process

The process of rating a bridge by PFEA includes four major steps which are briefly outlined below. These are discussed in greater detail by Schanck and Davids (2020). Although they were developed with the analysis of RC T-beam bridges as a main focus, as mentioned later, the concept is applicable to other types of slab-on-girder structures provided the appropriate constitutive models are used.

4.2.1 Moment-Curvature Relationship Extraction

The first step in PFEA is the extraction of the nonlinear moment-curvature relationships defining each girder's bending resistance when subjected to flexural loading up to and including failure. Starting from zero, a girder's section is subjected to a particular level of curvature and is discretized into n layers of equal thickness Compatibility is enforced by assuming strain in a layer to be proportional to curvature and height, and from these strains corresponding stresses are calculated. For the case of RC bridges, concrete is assumed to behave in compression as described by Hognestad (1951) with no strength in tension, and reinforcing steel is assumed to exhibit tension stiffening behavior, as suggested by Belarbi and Hsu (1994).

For a given level of curvature, Equation 2 is solved iteratively to determine the neutral axis location required for horizontal force equilibrium in the section under the current level of curvature, and Equation 3 is then used to compute the internal bending moment corresponding to the given curvature. In Equations 2 and 3, b_j is the width of the jth layer (either the width of the web or the flange, depending on the height of the layer from the bottom of the section, y_j and the presence of the feature), t is the layer thickness, f_{c_j} is the concrete stress in the jth layer, f_s and y_s are the stress in the reinforcing steel and the height of its centroid from the section bottom, and A_s is the cross-sectional area of the reinforcing steel. The process of iteratively solving Equation 2 and using Equation 3 to determine moment is repeated for increasing values of curvature until failure – defined by the concrete reaching its ultimate compressive strain of 0.003 at the extreme compression fiber (AASHTO 2012) – was reached. Figure 12 includes the extracted moment-curvature relationship for an interior girder from Bridge 5489 which is plotted as the blue curve.

$$\int \sigma dA \approx \left(\sum_{j=1}^{n} f_{c_j} b_j t \right) + f_s A_s = 0 \tag{2}$$

Investigation of Behavior of Skewed and Un-Skewed Reinforced Concrete T-Beam Bridges and Load Rating Improvement Through Proxy Finite Element Analysis

UMaine Composites Center Report 20-20-1613

$$\int \sigma y \, dA - M \approx \left(\sum_{j=1}^{n} f_{c_j} b_j y_j t \right) + f_s A_s y_s - M = 0 \tag{3}$$
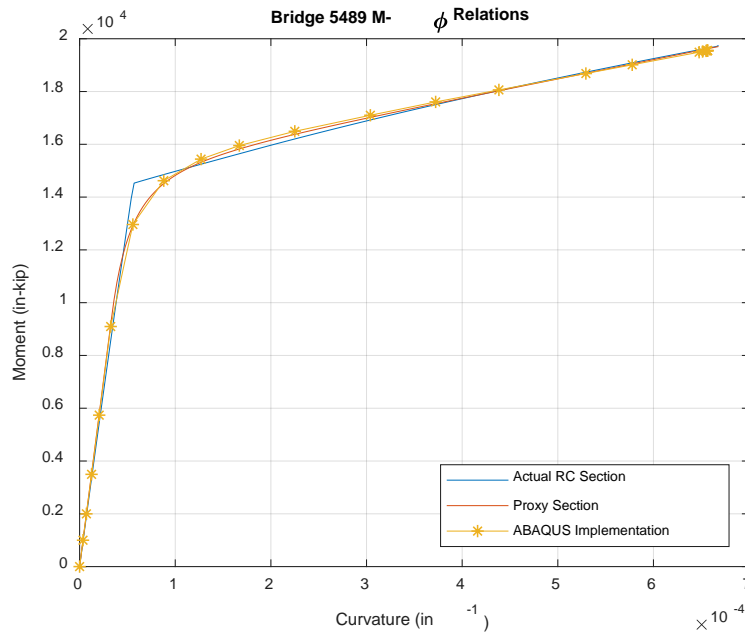
Figure 12: Moment Curvature Relationships for Bridge 5489 – Actual Section, Proxy Section, and ABAQUS Implementation

4.2.2 Proxy Section Creation

Once a section's moment curvature relationship has been extracted, a proxy section is developed that possesses an identical moment-curvature relationship to the actual section. In general, the overall geometry of the proxy section can be nearly the same as the actual section, but can be altered in order to facilitate modeling. However, the constitutive behavior of the proxy section is very much simplified in comparison to the actual section, significantly easing the difficulty of implementing complex constitutive models in a 3D finite-element model. For the bridges from this study, the proxy section consisted of a T-shaped section with a web and flange with geometry similar to the actual gross section.

To emulate the nonlinear moment-curvature relationship of the actual section, the proxy section's web was assigned elastic-perfectly plastic constitutive behavior, and the flange was assigned elastic behavior. The required material constants were determined by nonlinear optimization with a least-squares objective function defined by Equation 4 where f is a function of the optimization parameters x_i. The function f defines the proxy section's moment response when subjected to the curvatures used to find the real section's moment-curvature relationship, M are the values of

Investigation of Behavior of Skewed and Un-Skewed Reinforced Concrete T-Beam Bridges and Load Rating Improvement Through Proxy Finite Element Analysis

UMaine Composites Center Report 20-20-1613

bending moment from the actual RC section's moment-curvature relationship, and the double bars indicate the Euclidian norm. The function f applies a similar layered discretization technique as that used to determine the actual section's moment-curvature relationship while accounting for the proxy section's geometric and constitutive properties. For these bridges, a total of three variables (web elastic modulus, web yield stress, and flange elastic modulus) were optimized to fully define the proxy section since the geometry was assumed. However, more variables can be included to change geometric properties or add additional material properties if needed. Figure 12 shows the moment-curvature relation for a proxy section corresponding to an interior girder from Bridge 5489 as the red curve. As can be seen, the proxy section, with significantly simpler constitutive behavior, possesses a very similar moment-curvature relation to that of the actual section.

$$\lambda = \left\| f(x_1, x_2, \cdots x_j) - M \right\|_2 \tag{4}$$

It should be noted that the assumptions made in formulating proxy sections lead to one limitation of PFEA's broad use across a large range of bridge types. To this point, the bridges used in developing and verifying PFEA have had relatively thick decks and relatively close girder spacings. This has enabled the assumption of a linearly-elastic material model for the deck, both when optimizing proxy parameters, and in implementation into a FE model. This assumption may be less valid for bridges with thin decks or large girder spacing, which may experience a significant amount of material nonlinearity within their decks. Live-load data taken from such bridges would be needed to verify this limitation, and the limitation could then be addressed.

4.2.3 Finite Element Implementation

A FE analysis of a single girder with proxy section properties is conducted before it is synthesized into a full bridge model. This is done to verify that the implementation of the proxy section behaves appropriately, and allows fine-tuning of a failure strain parameter. This failure strain, when reached by any girder, causes the entire bridge to be considered failed and corresponds with concrete crushing. The individual girder models (as well as the full bridge models) are again implemented in ABAQUS and use S8R quadratic, reduced integration shell elements with 8 nodes and six degrees of freedom per node, to which appropriate geometric and material parameters are assigned. A convergence study revealed that a characteristic element length of around 3 in. consistently led to accurate results and so was used to form the mesh of individual girder models and full bridge models alike. The girders are simply supported with a known moment applied and resulting curvatures directly extracted from the results. Figure 12 shows the ABAQUS implementation of a proxy girder from Bridge 5489 as the yellow curve. As can be seen, the ABAQUS implementation agrees very well with both the theoretical proxy section and the actual section, showing that the implementation emulates the behavior of the actual section quite well.

Investigation of Behavior of Skewed and Un-Skewed Reinforced Concrete T-Beam Bridges and Load Rating Improvement Through Proxy Finite Element Analysis

UMaine Composites Center Report 20-20-1613

Full bridge PFEA models are constructed by placing the appropriate proxy girders side-by-side and tying adjacent flange degrees of freedom. Additionally, girder end-diaphragms are added between the webs of the proxy girders, which are modeled using S8R elements and whose geometry and material parameters were selected to ensure that their flexural rigidity was equal to those present in the actual bridges. Initially, intermediate diaphragms were also modeled. However, these tended to cause unrealistic stress concentrations which caused premature failure, and so were omitted thereafter, regardless of their presence on actual bridges. This omission aids in modeling, but also is conservative as it reduces bridges' ability to transversely distribute load. A meshed model of Bridge 3307 is presented in Figure 13. The models are simply supported and are configured with two loading steps: a dead load step in which a uniform dead-load pressure was applied to the entire deck, and a live-load step that would change depending on the loading required. This allows live-load effects to be isolated from dead-load effects while the entire loading history of the bridge, up to and including failure, is be applied.
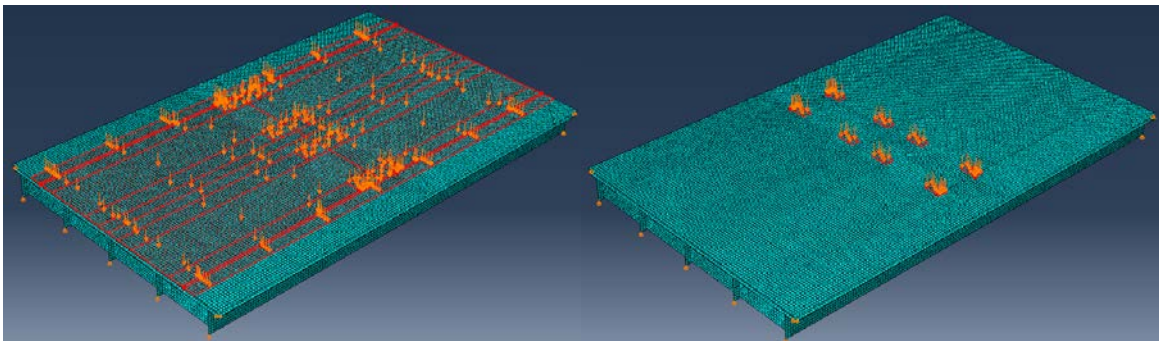
Figure 13: Bridge 3307 Full Proxy Bridge Model (Left: Showing Lane Load, Right: Showing Tandem Wheel Loads)

4.2.4 Analysis and Rating Factor Calculation

Live-loading is applied to match HL-93 notional loading with impact. Lane loads are applied to 10 ft wide strips of each lane as uniform pressures and HL-93 truck or tandem wheel loads are applied in both lanes. The wheel loads are positioned to produce maximum moment effects and are applied as pressure loads distributed over the tire contact pattern specified by AASHTO (2012) (over a 20 in. by 10 in. patch). Figure 13 includes the positions of both the lane and truck loads for illustration.

Rather than using a standard Newton-Raphson iterative solver to analyze the PFEA models, a Riks arc-length solver is employed (Riks, 1979). This allows *RF*s to be determined directly from the results of the model without prior knowledge of the load causing failure. At each iteration, the Riks solver used by ABAQUS scales the applied load by a load proportionality factor (*LPF*) and solves

Investigation of Behavior of Skewed and Un-Skewed Reinforced Concrete T-Beam Bridges and Load Rating Improvement Through Proxy Finite Element Analysis

UMaine Composites Center Report 20-20-1613

for the associated displacements. It then increases the *LPF* and continues to iterate until a stopping criterion is met, or the model becomes unstable. When a very large maximum *LPF* is used as the solver's termination criterion, the solver will increase *LPF* and solve for the next increment of displacement until one or more girders reaches their previously defined failure strains, at which point the model becomes unstable and the solver issues an analysis abort. This instability does not in itself hold physical significance, as it is purely numerical. The material damage model that initializes failure expects elements to gradually soften rather than immediately lose all stiffness, and as such the immediate loss of stiffness causes numerical ill-conditioning. However, as mentioned previously, the strain at which proxy section instability occurs directly corresponds with the strain causing top fiber crushing in the actual section, using their common moment-curvature relationship and assumption of linear strain distribution over the section depth. Therefore, the instability of the PFEA model is a direct mapping of the flexural failure of the actual bridge as defined by AASHTO, with the *LPF* causing that instability equal to the multiples of HL-93 loading causing the real bridge's flexural failure.

Using this basis, PFEA models can be used for load rating older bridges with while adhering to the AASHTO specifications. Equations 5 describe how a PFEA model can be used for bridge rating, where *RF* is the bridge's rating factor, ϕ is the AASHTO strength reduction factor (taken as 0.9 for under-reinforced concrete members in flexure), M_n is the bridge's moment capacity, γ_{DL} and γ_{LL} are the AASHTO dead-load and live load factors (taken as 1.25 and 1.35 respectively for operating conditions), M_{DL} and M_{LL} are the applied dead and live-load moments, respectively, and LPF_{max} is the maximum model-predicted *LPF*. The conventional capacity rating equation for individual members (taken from AASHTO (2011)) is given in Equation 5a, but used to describe the rating of the entire bridge acting as a system of interrelated members (as is seen in the behavior of actual structures and the PFEA model). Equation 5a is subsequently re-arranged in Equations 5b and 5c to solve for a term representing the maximum *LPF* predicted by the model, which can then be used to determine the *RF* with Equation 5d. This development shows that when dead-loading is applied to the model amplified by both the AASHTO dead-load factor and the inverse of the strength reduction factor, the bridge's *RF* can be computed that explicitly follows AASHTO guidelines for rating (2011) and analysis (2012). It should be noted that this rigorous consideration of load and resistance factor rating was not implemented in Schanck and Davids (2020).

$$RF = \frac{\phi M_n - \gamma_{DL} M_{DL}}{\gamma_{LL} M_{LL}} \tag{5a}$$

$$\frac{\gamma_{LL}}{\phi} RF * M_{LL} + \frac{\gamma_{DL}}{\phi} M_{DL} = M_n \tag{5b}$$

Investigation of Behavior of Skewed and Un-Skewed Reinforced Concrete T-Beam Bridges and Load Rating Improvement Through Proxy Finite Element Analysis

UMaine Composites Center Report 20-20-1613

$$\frac{\gamma_{LL}}{\phi} RF = \frac{M_n - \frac{\gamma_{DL}}{\phi} M_{DL}}{M_{LL}} = LPF_{max} \tag{5c}$$

$$RF = \phi \frac{LPF_{max}}{\gamma_{LL}} \tag{5d}$$

4.3 Results for Tested Bridges

The previously described PFEA rating process was applied to each of the 10 RC T-beam bridges that had been live-load tested in this study. The resulting flexural *RFs* are presented in Table 4, along with their original AASHTO determined *RFs*, and *RFs* updated by field live-load testing. As can be seen, PFEA resulted in significant increases in flexural *RF* for all bridges with respect to the original, AASHTO-determined *RFs*, and all but one saw additional increases relative to the *RFs* updated based on live-load testing. While some of these predictions seem optimistic, they are based solely on the mechanics of the problem at hand and assume nominal concrete compressive strength and steel yield strength, neglect any concrete tensile strength, and neglect of the effects of integral curbs, wearing surfaces, and railings. Additionally, they incorporate the load factors and strength reduction factors required by AASHTO for rating and design. Additionally, the truck or tandem loads applied to each land were offset longitudinally based on the bridges' angles of skew, further limiting the possible increases in *RF*.

Table 4: Flexural Rating Factors

Bridge	Skew (deg)	AASHTO Flexural RF	Field-Test Updated Flexural RF	PFEA Updated Flexural RF
2130	0	0.920	1.28	1.87
3307	0	0.920	1.61	1.30
3356	0	0.280	0.300	1.83
3776	0	0.690	1.20	1.43
5432	0	0.750	1.10	1.96
2390	30	0.757	0.838	1.56
2879	30	1.09	1.35	2.23
3848	30	0.887	1.15	1.72
5109	35	0.686	0.942	2.35
5489	15	0.784	1.10	1.91

As seen in Table 4, some of the increases in flexural *RF* are quite dramatic. However, the most dramatic is that of Bridge 3356, whose *RF* was increased by over 550% relative to its AASHTO *RF*. This seems overly optimistic, until the actual conditions of the bridge and the PFEA results are considered. The controlling *RF* for Bridge 3356 came from an extended, exterior girder that had been designed to carry a sidewalk but had been put into traffic service when the roadway was

Investigation of Behavior of Skewed and Un-Skewed Reinforced Concrete T-Beam Bridges and Load Rating Improvement Through Proxy Finite Element Analysis

UMaine Composites Center Report 20-20-1613

widened. Even after live-load testing, the bridge's *RF* could not be significantly increased because of the individual strength of that one girder. On the other hand, analysis with PFEA revealed a much less conservative prediction of the ultimate behavior of the bridge as a whole rather than as a collection of individual members. When loaded, the extended girder soon became nonlinear. However, because of the girder's ductility (captured accurately by the proxy section's moment-curvature relationship), this girder was able to deform inelastically with additional load being redistributed to the other girders. This continued until one of the interior girders reached its failure strain. In fact, the reported *RF* comes from an analysis in which the loads were moved as close to the exterior girder as was allowable, yet the girder was still able to avoid premature failure due to its ductility and the bridge's ability to redistribute load. This displays PFEA's ability to account for a bridge as a whole, allowing for realistic redistribution of load when nonlinearity is incurred and the ability to account for the ductility of lightly reinforced members.

4.4 Shear Effects

PFEA is intended to take advantage of the ductile, nonlinear behavior of slab-on-girder bridge girders (especially those of RC T-beam bridges) and the system behavior they exhibit at higher loads, up to and including ultimate flexural capacity. The beneficial nonlinear behavior of these bridges' girders do not readily extend to their response in shear, as their shear resisting mechanisms tend to be non-ductile. However, bridges' system responses do affect how shear load is distributed to individual girders, which can significantly affect the shear demand placed upon them. Since PFEA predicts the way in which a bridge works as a system to distribute loads, there is a potential to achieve a better understanding of shear demand through more realistic shear load distribution predicted by PFEA. The 10 bridges that had been live-load tested were therefore analyzed for shear with PFEA, with the aim of gaining additional understanding of the bridges' system response to shear loading.

The bridges' shear distributive response was investigated by analyzing two separate load cases: a case with loads applied to maximize shear, and one with loads arranged to maximize moment. To maximize shear, live loads that had been applied at the bridges' midspans were moved so that the rearmost load patches were applied one girder depth away from the bearing line. The bridges' dead loads and the lane load were kept in their original positions. These models were then analyzed with the resulting reaction forces at the loaded bearings assumed equal to the corresponding girders' maximum shear forces. To determine the shear resulting from loads positioned to maximize moment, the reaction forces from the original, moment-rating models were recovered and were again assumed equal to the maximum shear force in the respective girder.

In contrast to for the models used for flexural rating, the shear distribution models' *RF*s could not be automatically determined by the maximum achieved *LPF* from the Riks solver. Instead, the bridges' shear capacities were calculated based on AASHTO (2012) as implemented in a separate

Investigation of Behavior of Skewed and Un-Skewed Reinforced Concrete T-Beam Bridges and Load Rating Improvement Through Proxy Finite Element Analysis

UMaine Composites Center Report 20-20-1613

MATLAB function (provided in chapter A.2) which takes as input a model's dead-load and total dead and live-load reaction forces and reports each girder's resulting rating factor. AASHTO load and resistance factors were explicitly considered. These rating factors are presented in Table 5, along with the number of girders making up each bridge and the controlling girder (with girders numbered consecutively from one side to the other). It must be noted that these *RF*s are not necessarily representative of the capacities of the entire bridges. Because they assume maximum shear forces to be equal to reaction forces, they reflect capacity at girder ends only. In reality, the critical location for shear may be at a location away from the girders' ends, due to the girders' variable shear reinforcement spacing. For comparison, Table 5 also presents shear *RFs* calculated using the same MATLAB code, but using loads determined with AASHTO loading and distribution factors.

Table 5: Shear Rating Factors

Bridge	Skew (deg)	Number of Girders	AASHTO Shear *RF*	PFEA Shear *RF* – Moment Loading		PFEA Shear *RF* – Shear Loading	
				RF	Controlling Girder	*RF*	Controlling Girder
2130	0	4	1.71	2.87*	2/3	2.20	2/3
3307	0	5	1.32	2.11*	3	1.64	3
3356	0	6	1.14	2.84	4	1.55	3
3776	0	5	1.22	2.27*	3	1.19	3
5432	0	5	0.886	2.63	3	1.43	3
2390	30	5	0.650	1.80	5	1.21	3
2879	30	4	0.710	1.74	2	1.06	2
3848	30	5	0.560	2.00	5	1.22	3
5109	35	5	0.570	1.96	2	1.14	3
5489	15	5	0.726	2.18	3	1.11	3

*Bridge fails in flexure, larger loads cannot be applied

From the results presented in Table 5, difference in behavior between skewed and un-skewed bridges can be observed. For four of the five un-skewed bridges, the girder controlling the shear ratings was the center girder (or girders), which did not change with the positioning of the load. In the case of Bridge 3356, the controlling girder switched between two of the central girders as load was moved, and so can be thought to experience similar behavior, taking into account its unique geometry. Similar behavior can also be observed for Bridge 5489, which had the smallest angle of skew of the skewed bridges. For the remaining skewed bridges, a different behavior can be observed. When the loads were placed at midspan, the controlling girder for each of these bridges was an exterior girder or one of the non-central interior girders. These controlling girders correspond with the respective bridges' obtuse corners. However, when the loads are moved closer to the bearing line, each of these bridges' controlling girders shifted to their center girder (or one of the central girders in the case of Bridge 2390).

Investigation of Behavior of Skewed and Un-Skewed Reinforced Concrete T-Beam Bridges and Load Rating Improvement Through Proxy Finite Element Analysis

UMaine Composites Center Report 20-20-1613

The tendency for the obtuse corner bearing of a skewed bridge to attract additional load has been observed and documented in previous studies. For instance, Ebeido & Kennedy (1996) observed from scale models of slab-on-girder bridges that the bearing at the obtuse corner tended to attract much greater amounts of load for concentric load cases than the acute corner bearing, which they were able to simulate using FE analysis. Barr & Amin (2006), and Théoret et al. (2012) analyzed FE models of skewed slab-on-girder and flat-slab bridges (respectively), both noting that the obtuse corners tended to attract significant additional shear load. The results of this behavior were also observed during live-load testing of the skewed bridges, as discussed in detail above. This behavior arises as a result of the skewed bridges' geometries and the fact that the truck or tandem wheel loads used are not parallel to the angle of skew. When the loads on the more highly skewed bridges are distant from the bearing line, a significant amount of load is attracted to the bearing at the bridges' obtuse corners due to the shorter distance relative to the distance to interior bearings. However, when the loads are moved closer to the bearing line, much less load is attracted to that bearing due to the shorter distance to the center girder bearings. The prediction of this behavior by the PFEA models suggests that they are accurately predicting the system-behavior of the bridges, thus distributing shear load accurately.

As a final note, comparison of the PFEA and AASHTO shear *RFs* reveals additional insight into the differing accuracy between PFEA and AASHTO code-based predictions of shear load distribution for skewed bridges. For the un-skewed bridges, the AASHTO *RFs* are generally conservative relative to the PFEA *RFs*, but the disparity between them is not unreasonably large (with the exception of Bridge 3776, for which PFEA predicted a shear *RF* slightly lower than AASHTO). For each of these bridges, PFEA predicted a *RF* between 97.5% and 161% of AASHTO. Since the shear capacities for both *RF*s are calculated identically, this suggests that the AASHTO *DFs* for shear are reasonably accurate, yet conservative in describing shear load transfer. However, this is not the case for the skewed bridges. The AASHTO *RFs* for shear on the skewed bridges are very conservative relative to those calculated based on the results of PFEA, with PFEA predicting between 150% and 200% of AASHTO *RFs*. Again, given that shear capacities were calculated identically for AASHTO and PFEA ratings, these differences are largely due to shear load distribution. These differences suggest over-conservatism in AASHTO shear *DF*s or their skew correction factors which is not present in PFEA. This is consistent with findings reported by Barr and Amin (2006) who noted that AASHTO shear *DFs* to be conservative compared with the shear load distribution inferred by linearly elastic finite element analysis. Because PFEA treats bridge models as systems rather than individual members, it can accurately simulate distribution of shear force in skewed bridges, leading to better predictions of shear rating. However, these predictions should also remain reasonably conservative as they use girder capacities calculated with AASHTO specifications (2012).

Investigation of Behavior of Skewed and Un-Skewed Reinforced Concrete T-Beam Bridges and Load Rating Improvement Through Proxy Finite Element Analysis

UMaine Composites Center Report 20-20-1613

4.5 Consideration of AASHTO Specifications

As shown above, analysis of bridges by PFEA can provide a more accurate assessment of bridge behavior than conventional beam-line analysis, tracking both ductility and load redistribution up to and including failure. However, for the technique to be acceptable in practice, it must reflect the standards and specifications governing bridge design and assessment, namely the AASHTO *LRFD Bridge Design Specifications* (2012) and *Manual for Bridge Evaluation* (2011). This section explicitly addresses PFEA's adherence to the practices allowed by the standards, and addresses the few discrepancies that exist. The three general steps of load rating by PFEA – moment-curvature relation extraction; development of proxy sections; and analysis with the finite element method – will be addressed, and it is shown that the techniques used in PFEA are generally allowable under the current code and/or abide by the letter and spirit of the current code.

Extraction of moment-curvature relationships as a method of member analysis is a well-accepted method and is fully allowed in the current AASHTO specifications (2012). The code specifies that, "[a]ny method of analysis that satisfies the requirements of equilibrium and compatibility and utilizes stress-strain relationships for the proposed materials may be used" (AASHTO 2012, 4.4). As described above, PFEA moment-curvature extraction ensures equilibrium of internal forces and moments, and uses conventional beam theory assumptions to ensure strain compatibility through the section. Additionally, stress-strain relations are used for both concrete and reinforcing steel. The relation used for concrete, that proposed by Hognestad (1951), is fully acceptable by the code which allows stress distributions which are, "assumed to be rectangular, parabolic, or any other shape that results in a prediction of strength in substantial agreement with the test results" (AASHTO 2012, 5.7.2.1). The use of a concrete crushing strain of 0.003 is generally conservative and in line with AASHTO for bridges in good condition, like those tested here. For bridges in poorer condition whose ductility is in doubt, reduction of the concrete crushing strain (to 0.002 for instance) will effectively reduce predicted girder ductility, thus reducing the PFEA model's ability to redistribute load and increase the conservatism in the analysis.

The constitutive relation for steel proposed by Belarbi and Hsu (1994) and utilized by PFEA is not explicitly allowed by AASHTO, but is widely accepted in the literature. Although the relation represents a "stress-strain curve representative of the steel" (AASHTO 2012, 5.7.2.1), it leads to ultimate moment capacities in excess of those determined assuming an elastic-perfectly plastic model, which may cause some concern. To ease this concern, moment-curvature analysis (using both the Hognestad (1951) concrete and Belarbi and Hsu (1994) reinforcing steel constitutive models) was used to reproduce test data of actual RC beam failure tests, providing evidence of the model's applicability. Moment-curvature relationships for the control beams described by Loring and Davids (2015) and beams by Xing et al. (2010) were extracted and used to predict load-deflection behavior. Deflection was predicted numerically using a 5th order boundary-value problem solver in MATLAB to solve the nonlinear beam differential equation. Figures 14 and 15

Investigation of Behavior of Skewed and Un-Skewed Reinforced Concrete T-Beam Bridges and Load Rating Improvement Through Proxy Finite Element Analysis

UMaine Composites Center Report 20-20-1613

show the behavior predicted from the moment-curvature relationships compared with the measured load-displacement data. As is clear, the load deflection behavior predicted matches the measured behavior quite well. In addition, if required, the maximum predicted moment of a girder can be reduced in moment-curvature extraction by reducing the assumed yield stress of the steel. This would have the effect of reducing the maximum moment supported by a girder, without greatly affecting its ductility. The yield stress used could be tuned such that the maximum predicted moment equaled the maximum moment determined by conventional analysis.
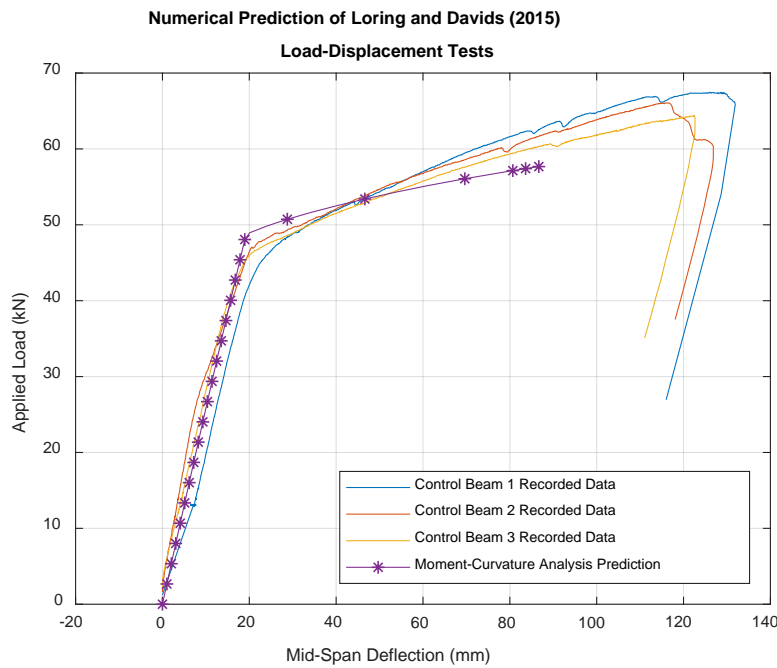

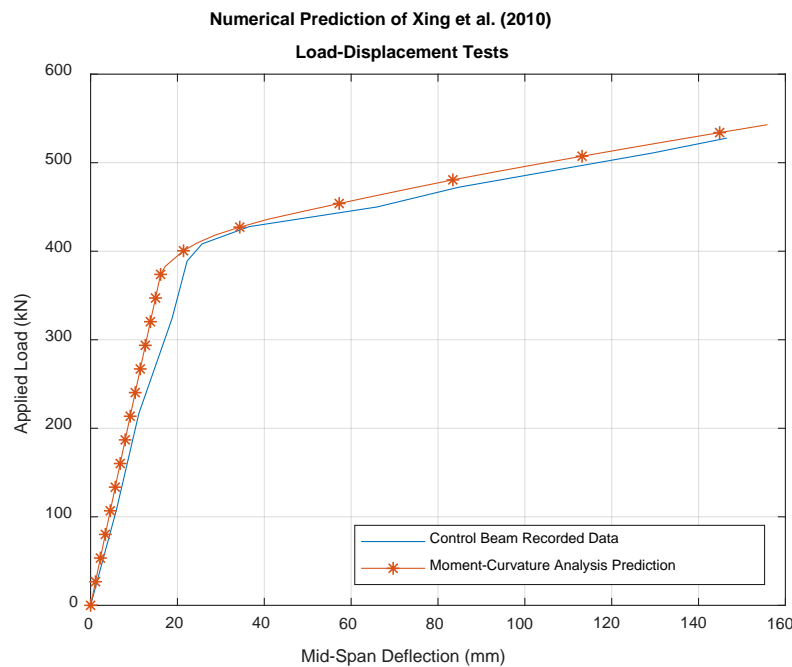Figure 14: Comparison of Predicted and Measured Load-Deflection Behavior from Loring and Davids (2015)

Investigation of Behavior of Skewed and Un-Skewed Reinforced Concrete T-Beam Bridges and Load Rating Improvement Through Proxy Finite Element Analysis

UMaine Composites Center Report 20-20-1613

Figure 15: Comparison of Predicted and Measured Load-Deflection Behavior Xing et al. (2010)

The creation of proxy sections to represent a bridge's actual girders is not specifically addressed by AASHTO (2012), does falls under the analysis category of "Equivalent Members" defined in section 4.5.5 given below.

> Components or groups of components of bridges with or without variable cross-sections may be modeled as a single equivalent component provided that it represents all the stiffness properties of the components or group of components. The equivalent stiffness properties may be obtained by closed-form solutions, numerical integration, submodel analysis, and series and parallel analogies.

Modeling real girders with proxy sections is consistent with this provision. The stiffness characteristics of the real girders are determined by numerical integration, which are then given to the proxy sections based on the results of nonlinear optimization. Proxy sections mimic all of the relevant stiffness and strength characteristics required for flexural analysis of the actual section and thus are a valid option.

Finally, the use of 3D, nonlinear FE models for analysis is accepted by AASHTO, and the model formulation explicitly considers the requirements for bridge rating factor evaluation. As mentioned above, AASHTO specifies that "[a]ny method of analysis that satisfies the requirements of equilibrium and compatibility and utilizes stress-strain relationships for the proposed materials may be used" (AASHTO 2012, 4.4), and specifically lists FE analysis as an example of an

Investigation of Behavior of Skewed and Un-Skewed Reinforced Concrete T-Beam Bridges and Load Rating Improvement Through Proxy Finite Element Analysis

UMaine Composites Center Report 20-20-1613

approved analysis technique. In addition, the use of inelastic material behavior (4.5.2.3) and geometric nonlinearity (4.5.3.2) are explicitly allowed, solidifying the models' formulations. Finally, as discussed and presented in Equations 5, the application of dead loads and live-loads are formulated such that *RF*s governed by AASHTO (2011) can easily be computed while incorporating the requisite strength reduction factors, load factors, and impact factors.

4.6 Current and Future Development

In its current state, PFEA has been shown to produce what appear to be realistic estimates of simple-span RC T-beam bridge *RFs*. It has shown utility for both un-skewed and skewed bridges as seen in the results displayed in Tables 4 and 5. PFEA is currently being tested against the results of a RC T-beam bridge tested to failure by Burdette and Goodpasture (1971) to provide additional verification of its accuracy. In addition, PFEA is being extended to account for prestressing such that it may be used to analyze prestressed concrete bridges. The technique could also be extended to cover steel-girder bridges and continuous bridges, and be integrated into a self-contained program used to increase the accuracy of ratings for older girder bridges.

5 Summary and Conclusions

5.1 Skewed and Un-Skewed Bridge Behavioral Differences

Live-load testing of five un-skewed and five skewed RC T-beam bridges allowed their behaviors to be directly compared under reasonably similar conditions, and two main differences to be identified. Through calibration and simulation using linear FE models, the bridges' behaviors and possible causes for these behaviors could be further explored, with results extending beyond those revealed by testing alone.

The strain data collected during live-load testing showed a tendency for skewed bridges' load distribution to have a much greater dependence on load positioning than did similar un-skewed bridges, as shown by *GLFs* calculated using recorded mid-span strains. Using the calibrated, linear FE models, the reaction forces between the girders and abutments were recovered. This confirmed that the skew bridges' high dependence on transverse load positioning is likely due to the shortened distance to obtuse corners, which in-turn attracts a greater amount of load. The same live-load tests also revealed skewed bridges' much greater susceptibility to unintended end fixity, indicated by negative strains recorded at girder ends. The linear FE models revealed the skewed bridges' tendency to undergo warping displacements. These predicted displacements, along with observations of the bridges' actual bearing conditions led to the hypothesis of skewed bridges' tendency to collect debris between the abutment and backwall, restricting their displacement and inducing negative strains.

Investigation of Behavior of Skewed and Un-Skewed Reinforced Concrete T-Beam Bridges and Load Rating Improvement Through Proxy Finite Element Analysis

UMaine Composites Center Report 20-20-1613

These observations and associated explanations, while important to furthering the understanding of actual bridges' behaviors, also can be practically useful when considering a bridge for permitting and load-rating. They are also useful and when evaluating the results of future live-load testing of similar bridges. For instance, noting the dependence of skewed T-beam bridge response on transverse load positioning for load distribution can inform decisions on permit-load planning, particularly whether overweight loads should be carried in normal travel lanes or whether they should be centered, with other traffic temporarily stopped or diverted. Additionally, live-load test results revealed some unintended end-fixity for skewed T-beam bridges which was not observed for the un-skewed bridges. This appears to be due to debris fouling the bearings, which was more apparent for the skewed bridges.

5.2 Proxy Finite Element Analysis

A novel, nonlinear FE analysis technique, PFEA, has been developed for the purpose of load-rating older bridges with a higher level of accuracy than is available through standard engineering analysis. It condenses the complex flexural behavior of a bridge girder into a single, nonlinear relationship describing its curvature response when subjected to an external moment. This relationship is then used to develop a proxy section that maintains the actual section's moment-curvature relationship, but can have a much simpler geometries and can use much simpler constitutive models. Proxy sections are assembled into full bridge models loaded by factored dead-load and HL-93 live-load. Solutions are achieved using a Riks arc-length algorithm which continues to increase applied load until the model becomes unstable, signifying capacity of the bridge has been reached.

PFEA was used to update the load ratings of each of the ten RC T-beam bridges tested as a part of this study with promising results. The *RFs* for each bridge were able to be increased relative to the *RFs* calculated using standard AASHTO provisions, and *RFs* for nine of the ten were increased relative to the results from live-load testing. An important observation from these results is that, although they seem optimistic, they rely solely on well-established mechanics principles and incorporate conservative assumptions that limit the technique's possible benefit. Notably, the technique is able to account for both the entire, nonlinear moment-curvature response of individual girders to take advantage of their ductility, and the bridge system's ability to redistribute load to more lightly loaded girders when others become nonlinear. The technique is also able to provide some additional insight into bridges' behavior under shear, as it allows realistic distribution of load effects (both moment and shear) to individual girders based on load position, geometry, and material nonlinearity. With continued development, this technique has the potential to improve the *RFs* of older bridges that are known to carry modern loading without distress despite having low *RFs* based on conventional engineering analysis.

Investigation of Behavior of Skewed and Un-Skewed Reinforced Concrete T-Beam Bridges and Load Rating Improvement Through Proxy Finite Element Analysis

UMaine Composites Center Report 20-20-1613

6   References

1. AASHTO (2011). *The Manual for Bridge Evaluation.* American Association of State Highway and Transportation Officials, Washington DC.

2. AASHTO (2012). *AASHTO LRFD Bridge Design Specifications*. American Association of State Highway and Transportation Officials, Washington DC.

3. *ABAQUS 6.13* [Computer software]. Vélizy-Villacoublay, France, Dassault Systèmes.

4. Albraheemi, M.J.A., Davids, W.G., Schanck, A., & Tomlinson, S. (2019). Evaluation and rating of older non-composite steel girder bridges using field live load testing and nonlinear finite element analysis. *Bridge Struct.* 15(1-2). 27-41.

5. Barr, P.J., & Amin, MD., N. (2006). Shear live-load distribution factors for I-girder bridges. *J. of Bridge Eng.* 11(2). 197-204.

6. Buckle, I.G., Dickson, A.R., & Phillips, M.H. (1985). Ultimate strength of three reinforced concrete highway bridges. *Can. J. of Civ. Eng*. 12, 63-72.

7. Burdette, E.G., & Goodpasture, D.W. (1971). Final Report for "Full-Scale Bridge Testing". University of Tennessee, Knoxville, TN.

8. Belarbi, A. & Hsu, T.T.C. (1994). Constitutive laws of concrete in tension and reinforcing bars stiffened by concrete. *ACI Struct. J.,* July-August, 465-74.

9. Ebeido, T. & Kennedy, J.B. (1996). Shear and reaction distributions in continuous skew composite bridges. *J. of Bridge Eng.* 1(4). 155-65.

10. Hognestad, E. (1951). *A study of combined bending and axial load in reinforced concrete members.* Urbana, IL.: University of Illinois, Urbana.

11. Loring, H.B., & Davids, W.G. (2015). Mechanically fastened composite strips for flexural strengthening of concrete beams. *Constr. and Build. Mater.*, 76, 118-29.

12. Riks, E. (1979). An incremental approach to the solution of snapping and buckling problems. *Int. J. of Solids and Struct.*, 15(7), 529-51.

13. Saraf, V. (1998). Evaluation of existing RC slab bridges. *J. of Perform. of Constr. Facil.*, 12(1), 20-4.

14. Schanck, A. & Davids, W. (2018a). *Live Load Testing and Load Rating of Five Reinforced Concrete T-Beam Bridges.* Orono, ME.: University of Maine.

15. Schanck, A. & Davids, W. (2018b). *Live Load Testing and Load Rating of Five Skewed Reinforced Concrete T-Beam Bridges.* Orono, ME,: University of Maine.

16. Schanck, A. & Davids, W. (2020). Capacity assessment of older T-beam bridges by nonlinear proxy finite element analysis. *Struct.* 23(2020), 267-78.

Investigation of Behavior of Skewed and Un-Skewed Reinforced Concrete T-Beam Bridges and Load Rating Improvement Through Proxy Finite Element Analysis

UMaine Composites Center Report 20-20-1613

17. Théoret, P., Massicotte, B., & Conciatori, D. (2012). Analysis and design of straight and skewed slab bridges. *J. of Bridge Eng.* 17(2). 289-301.

18. Xing, G., Wu, Tao, Liu, B., Huang, H., & Gu, S. (2010). Experimental investigation of reinforced concrete T-beams strengthened with steel wire mesh embedded in polymer mortar overlay. *Adv. in Struct Eng*. 13(1): 69-79.

Investigation of Behavior of Skewed and Un-Skewed Reinforced Concrete T-Beam Bridges and Load Rating Improvement Through Proxy Finite Element Analysis

UMaine Composites Center Report 20-20-1613

A.1   Supplementary Figures

A.1.1 Live-Load Test Girder Lane Fraction Plots
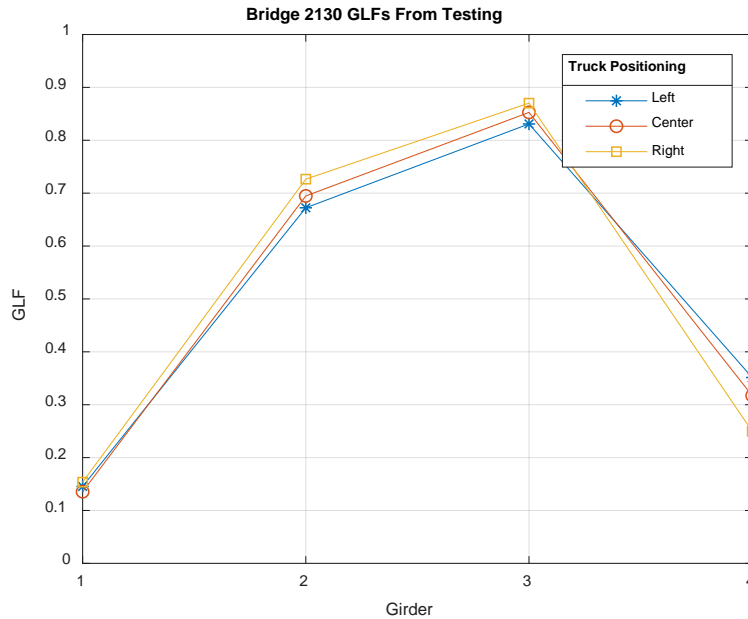
Figure 16: GLFs Calculated from Live-Load Testing – Bridge 2130 (Un-Skewed)
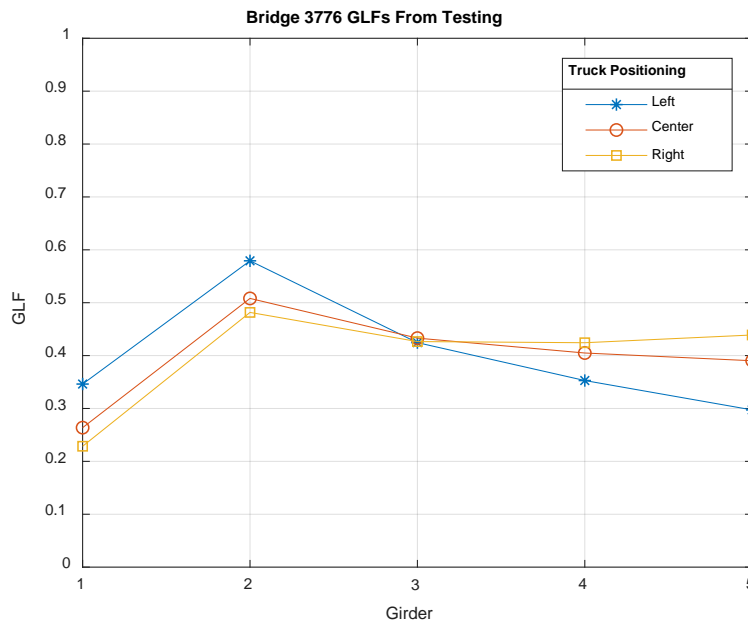
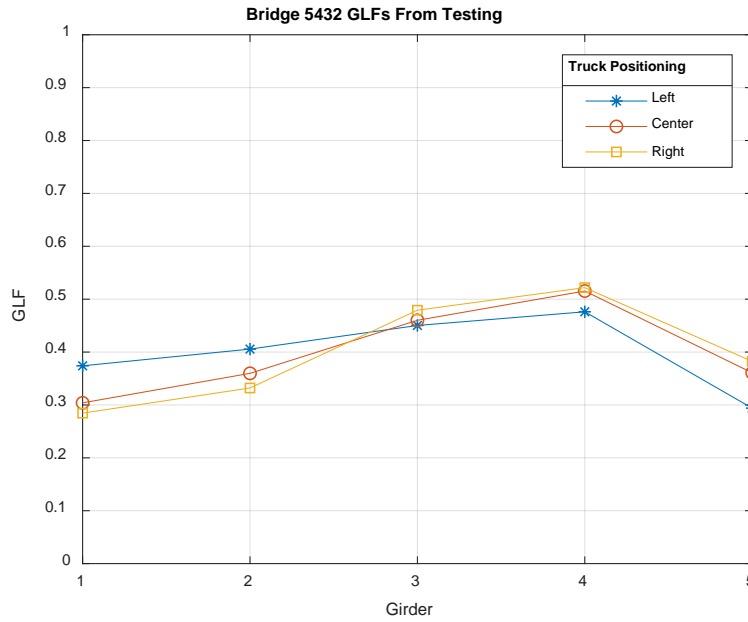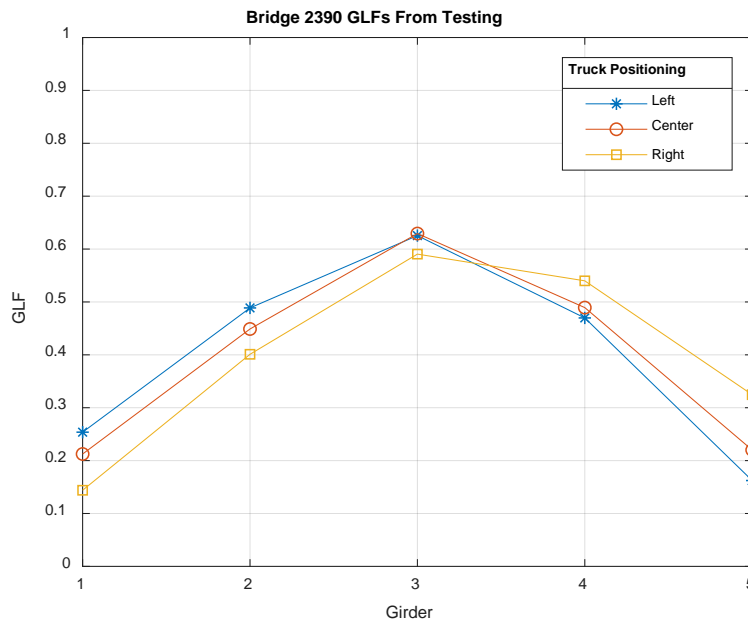Figure 17: GLFs Calculated from Live-Load Testing – Bridge 3776 (Un-Skewed)

Investigation of Behavior of Skewed and Un-Skewed Reinforced Concrete T-Beam Bridges and Load Rating Improvement Through Proxy Finite Element Analysis

UMaine Composites Center Report 20-20-1613

Figure 18: GLFs Calculated from Live-Load Testing – Bridge 5432 (Un-Skewed)

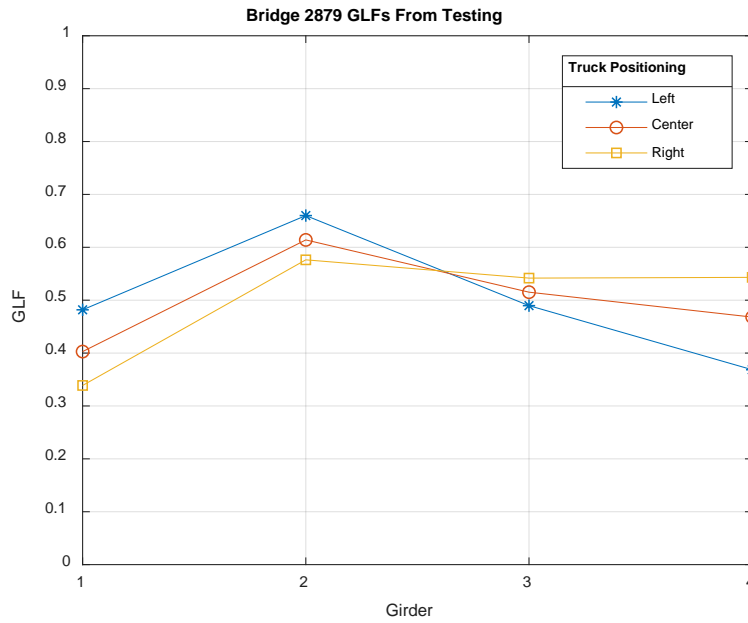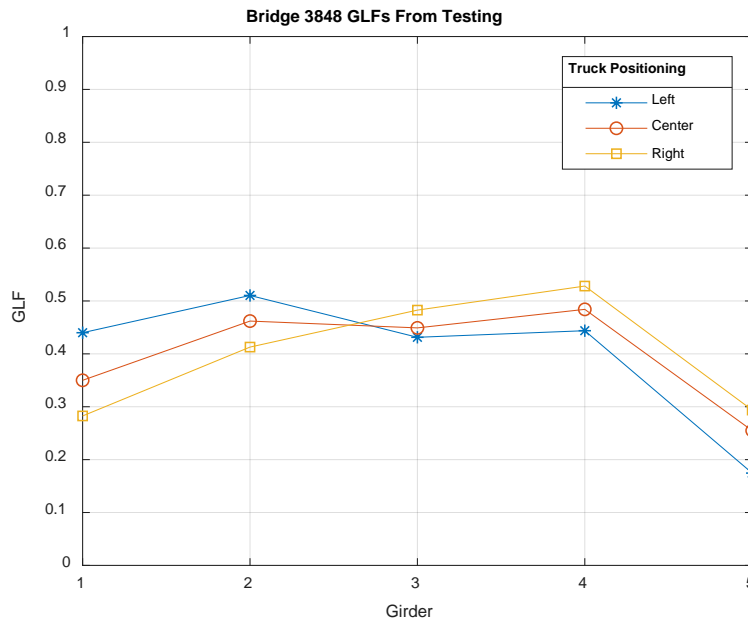Figure 19: GLFs Calculated from Live-Load Testing – Bridge 2390 (Skewed)

Investigation of Behavior of Skewed and Un-Skewed Reinforced Concrete T-Beam Bridges and Load Rating Improvement Through Proxy Finite Element Analysis

UMaine Composites Center Report 20-20-1613

Figure 20: GLFs Calculated from Live-Load Testing – Bridge 2879 (Skewed)

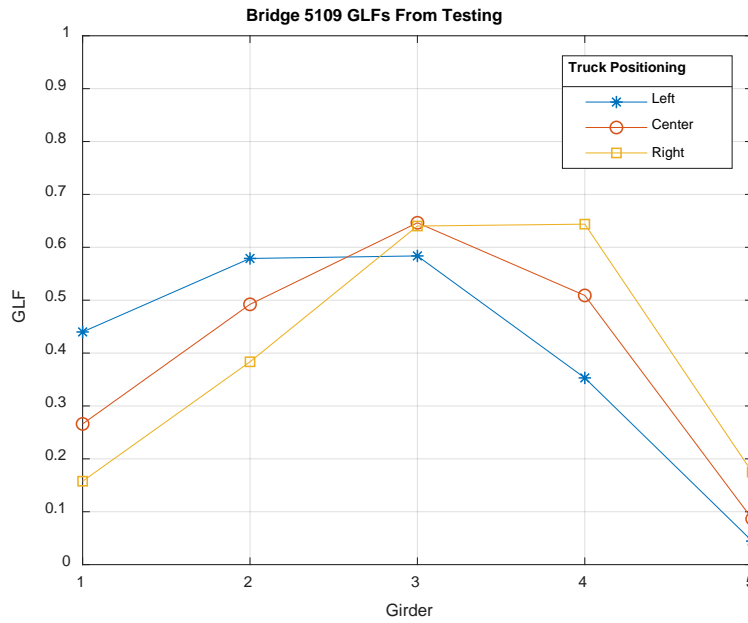Figure 21: GLFs Calculated from Live-Load Testing – Bridge 3848 (Skewed)

Investigation of Behavior of Skewed and Un-Skewed Reinforced Concrete T-Beam Bridges and Load Rating Improvement Through Proxy Finite Element Analysis

UMaine Composites Center Report 20-20-1613

Figure 22: GLFs Calculated from Live-Load Testing – Bridge 5109 (Skewed)

Investigation of Behavior of Skewed and Un-Skewed Reinforced Concrete T-Beam Bridges and Load Rating Improvement Through Proxy Finite Element Analysis

UMaine Composites Center Report 20-20-1613

A.1.2 Fractions of Reaction Force from Linear Finite Element Analysis
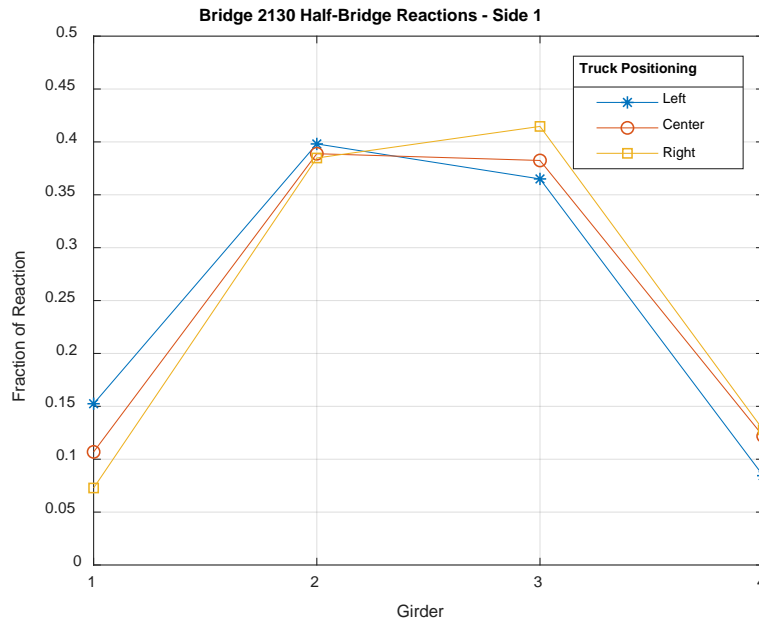
Figure 23: Fractions of Reaction Force Attracted to Each Support at Side 1 – Bridge 2130 (Un-Skewed)
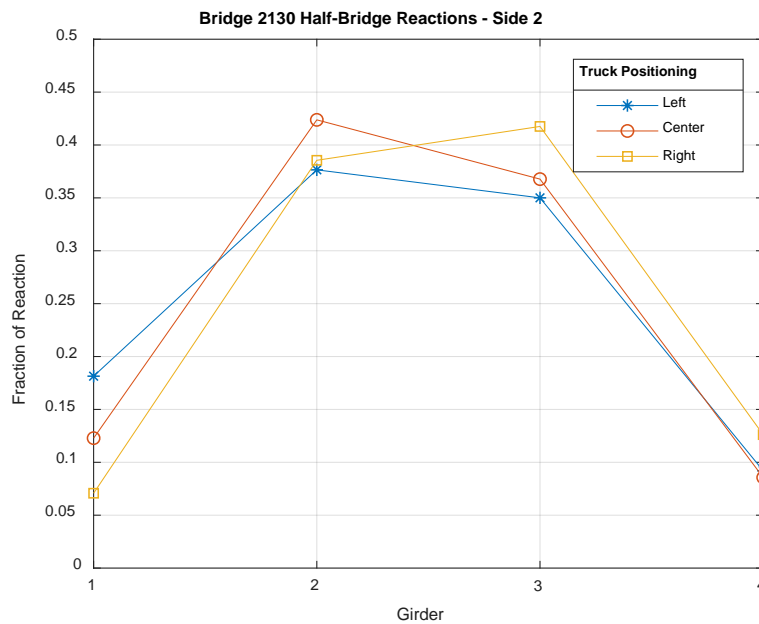

Figure 24: Fractions of Reaction Force Attracted to Each Support at Side 2 – Bridge 2130 (Un-Skewed)
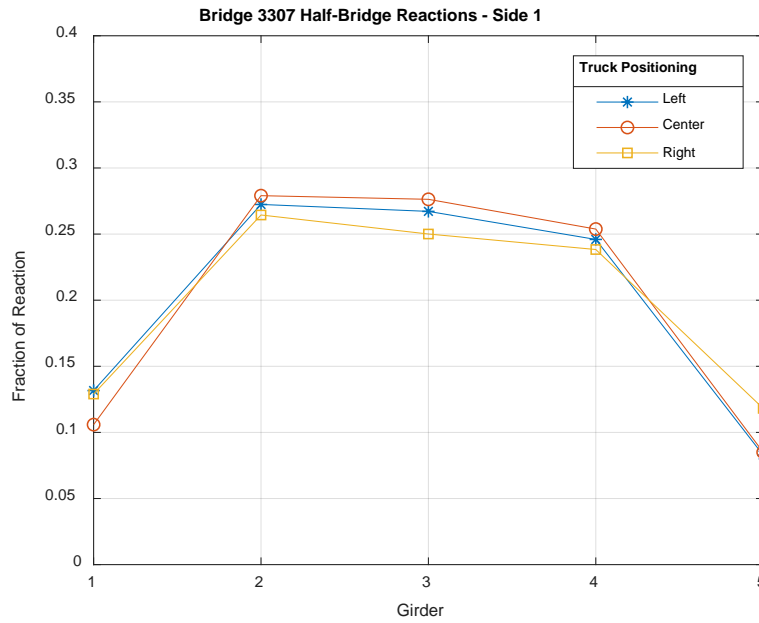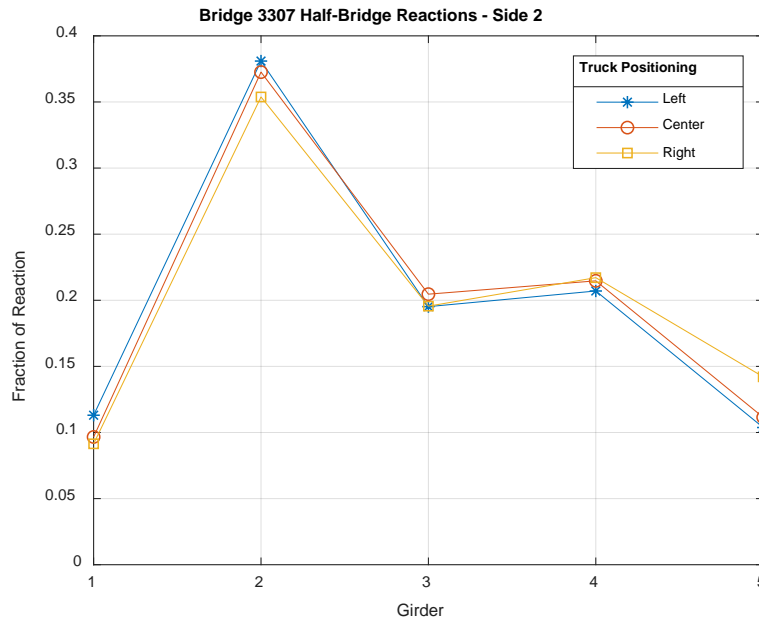
Investigation of Behavior of Skewed and Un-Skewed Reinforced Concrete T-Beam Bridges and Load Rating Improvement Through Proxy Finite Element Analysis

UMaine Composites Center Report 20-20-1613

Figure 25: Fractions of Reaction Force Attracted to Each Support at Side 1 – Bridge 3307 (Un-Skewed)

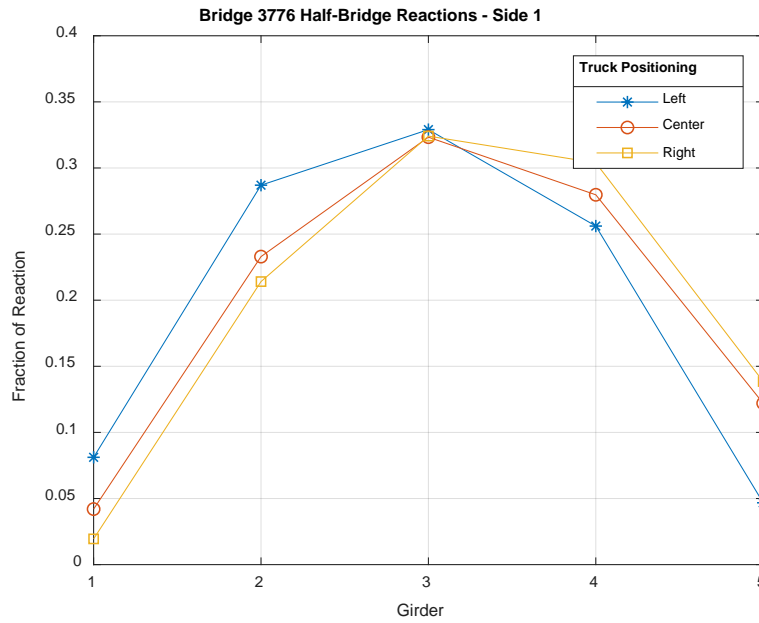Figure 26: Fractions of Reaction Force Attracted to Each Support at Side 2 – Bridge 3307 (Un-Skewed)

Investigation of Behavior of Skewed and Un-Skewed Reinforced Concrete T-Beam Bridges and Load Rating Improvement Through Proxy Finite Element Analysis

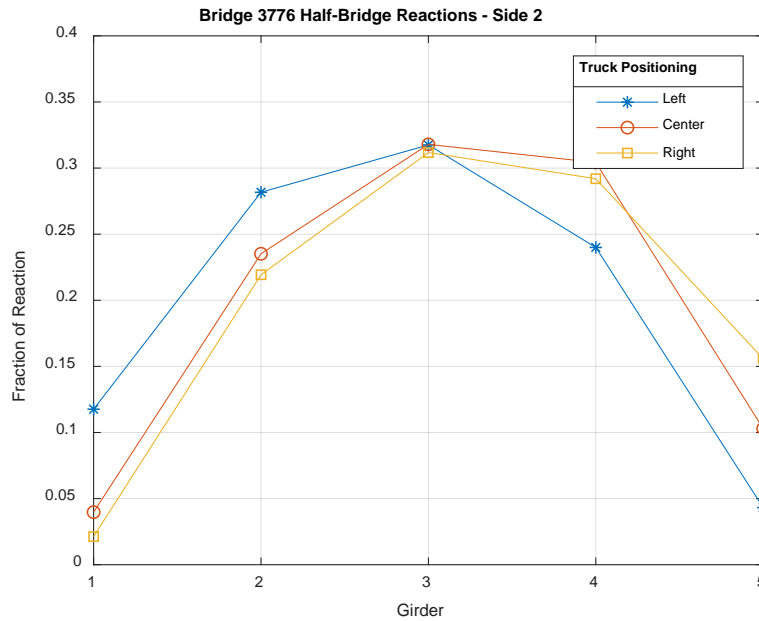*UMaine Composites Center Report 20-20-1613*

Figure 27: Fractions of Reaction Force Attracted to Each Support at Side 1 – Bridge 3776 (Un-Skewed)

Figure 28: Fractions of Reaction Force Attracted to Each Support at Side 2 – Bridge 3776 (Un-Skewed)

Investigation of Behavior of Skewed and Un-Skewed Reinforced Concrete T-Beam Bridges and Load Rating Improvement Through Proxy Finite Element Analysis

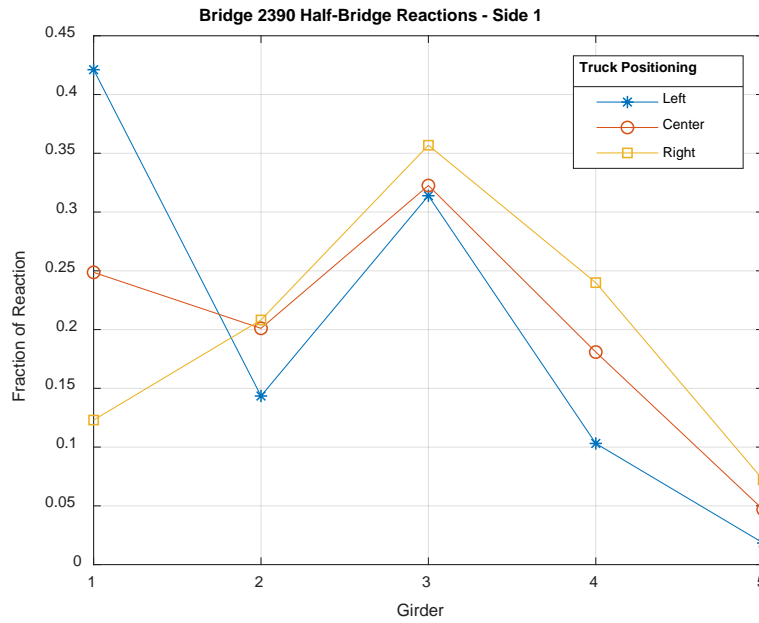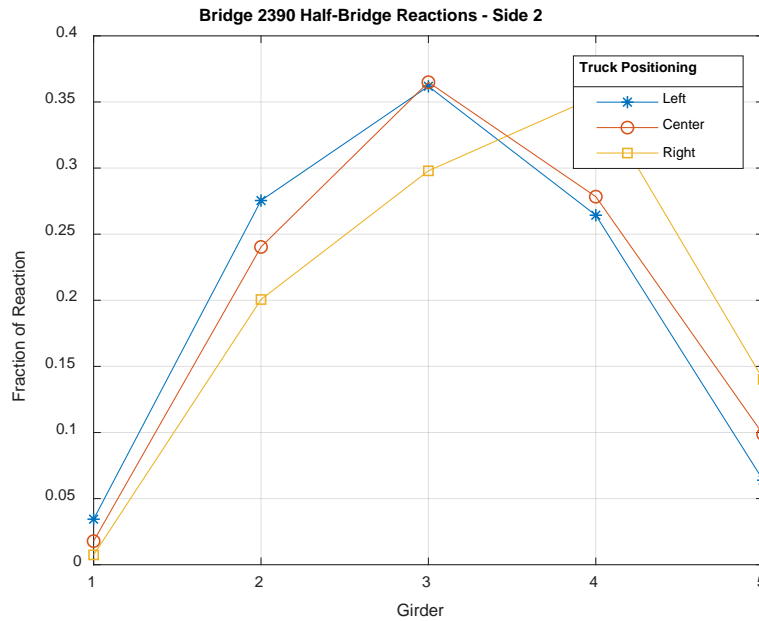*UMaine Composites Center Report 20-20-1613*

Figure 29: Fractions of Reaction Force Attracted to Each Support at Side 1 – Bridge 2390 (Skewed)

Figure 30: Fractions of Reaction Force Attracted to Each Support at Side 2 – Bridge 2390 (Skewed)

Investigation of Behavior of Skewed and Un-Skewed Reinforced Concrete T-Beam Bridges and Load Rating Improvement Through Proxy Finite Element Analysis

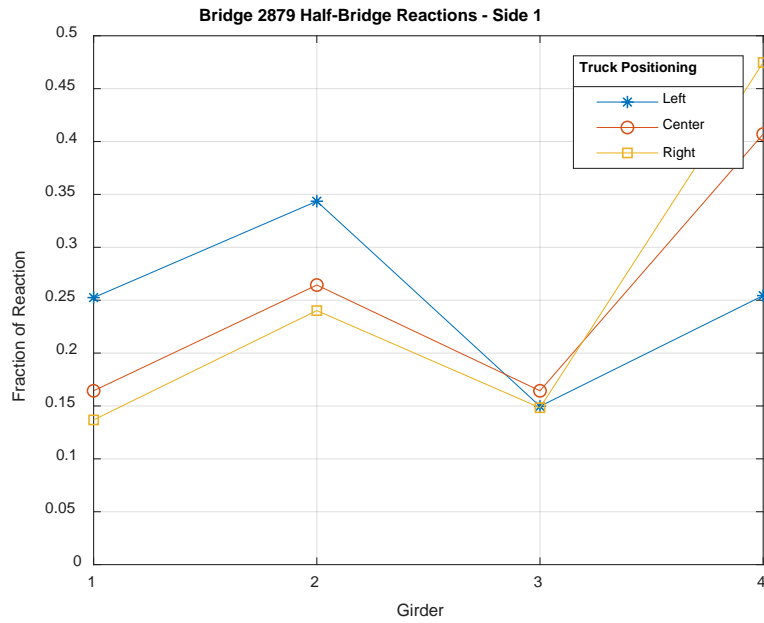*UMaine Composites Center Report 20-20-1613*

Figure 31: Fractions of Reaction Force Attracted to Each Support at Side 1 – Bridge 2879 (Skewed)

Figure 32: Fractions of Reaction Force Attracted to Each Support at Side 2 – Bridge 2879 (Skewed)
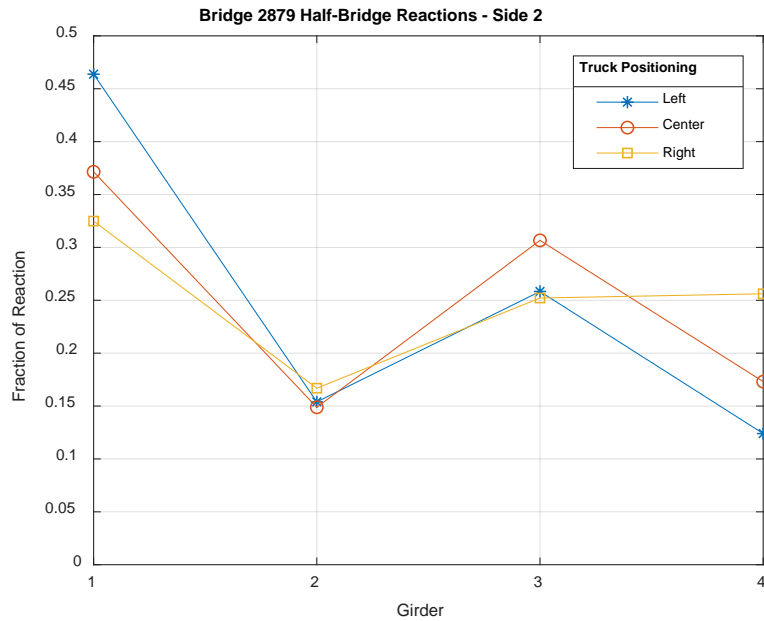
Investigation of Behavior of Skewed and Un-Skewed Reinforced Concrete T-Beam Bridges and Load Rating Improvement Through Proxy Finite Element Analysis

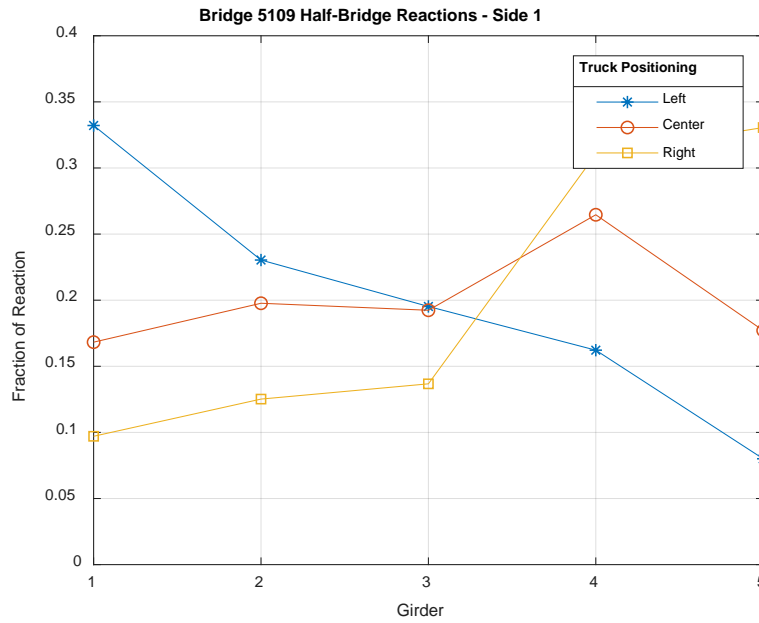*UMaine Composites Center Report 20-20-1613*

Figure 33: Fractions of Reaction Force Attracted to Each Support at Side 1 – Bridge 5109 (Skewed)

Figure 34: Fractions of Reaction Force Attracted to Each Support at Side 2 – Bridge 5109 (Skewed)

Investigation of Behavior of Skewed and Un-Skewed Reinforced Concrete T-Beam Bridges and Load Rating Improvement Through Proxy Finite Element Analysis

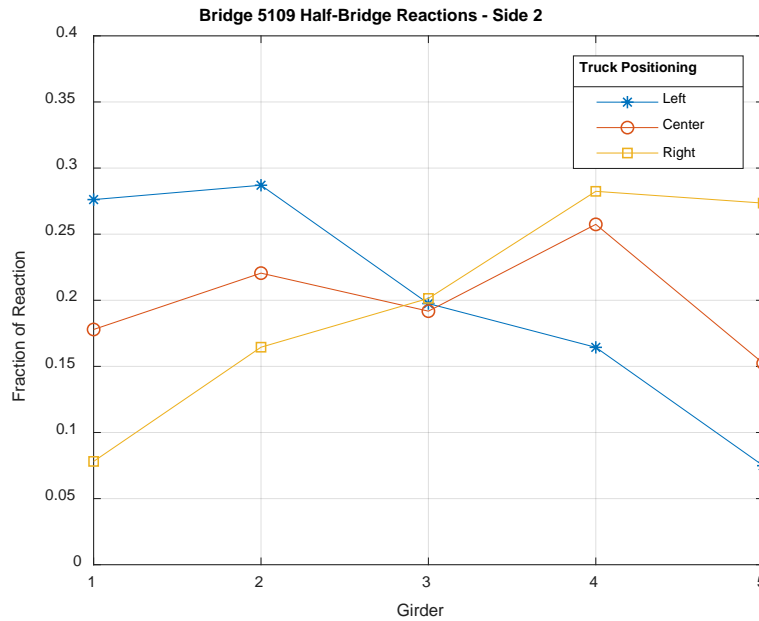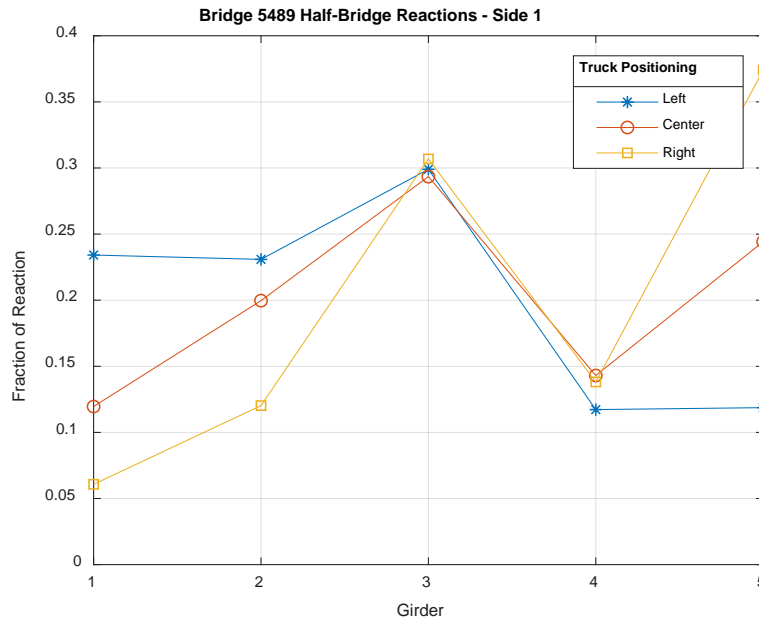*UMaine Composites Center Report 20-20-1613*

Figure 35: Fractions of Reaction Force Attracted to Each Support at Side 1 – Bridge 5489 (Skewed)

Figure 36: Fractions of Reaction Force Attracted to Each Support at Side 2 – Bridge 5489 (Skewed)
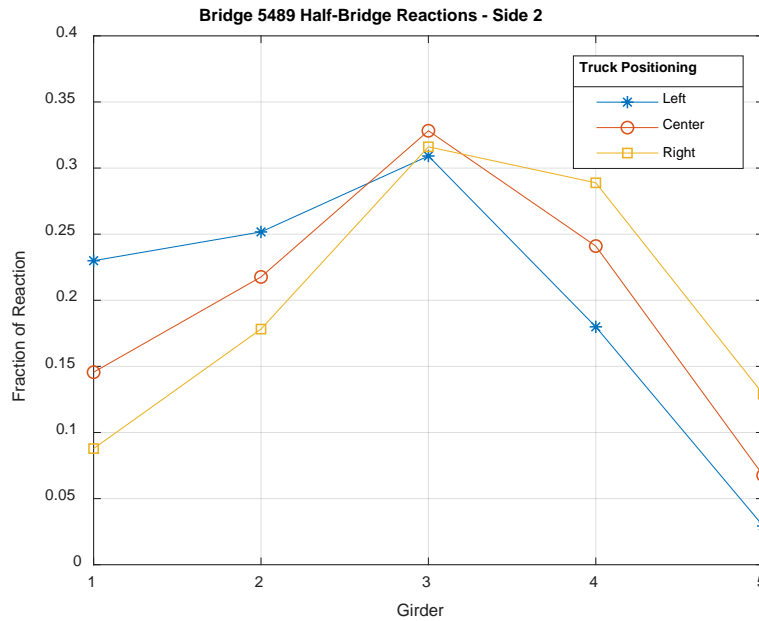
Investigation of Behavior of Skewed and Un-Skewed Reinforced Concrete T-Beam Bridges and Load Rating Improvement Through Proxy Finite Element Analysis

UMaine Composites Center Report 20-20-1613

A.2   Shear Rating MATLAB Code

Investigation of Behavior of Skewed and Un-Skewed Reinforced Concrete T-Beam Bridges and Load Rating Improvement Through Proxy Finite Element Analysis

UMaine Composites Center Report 20-20-1613

Contents

```
function RF = PFEA_shear(total_rxn,DL_rxn)
```

```
% This fuction takes the maximum reaction forces recovered from a PFEA
% flexural rating analysis and calculates the shear rating based on AASHTO
% calculated shear capacities. The total reaction force and the reaction
% force due to dead load only are inputs (both in units of kip).

% All calculations based on AASHTO LRFD Bridge Design Guide (2012)

% Andrew Schanck
% 10/2/2019
```

Inputs

```
% Shear reinforcement area (in^2)
Av = [.393 .393 .393 .393 .393];
% Steel yield stress (ksi)
fy = 33;
% T-beam web width (in)
bv = [20 20 20 20 20];
% T-beam height (in)
h = [35.75 35.75 35.75 35.75 35.75];
% Height of longitudinal steel centroid at girder end (in)
ys = [3.125 3.125 3.125 3.125 3.125];
% Depth of longitudinal steel (in)
de = h-ys;
% Steel elastic modulus (ksi)
Es = 29000;
% Area of longitudinal steel at girder end (in^2)
As = [5.0625 5.0625 5.0625 5.0625 5.0625];
% Concrete compressive strength (ksi)
fpc = 2.5;
% Stirrup spacing (in)
s = [12 12 12 12 12];
% Live load factor
load_factor = 1.35;
% Girder end moment resistance (in-kip)
Mn = [4987.7 5364.4 5364.4 5364.4 4987.7];
% Calculate live-load shear (kip)
rxn = total_rxn-DL_rxn;
% Make sure that the expected number of reactions is provided
if length(rxn) ~= length(Av)
    error('Must have as many ractions as girders.')
end
```

Investigation of Behavior of Skewed and Un-Skewed Reinforced Concrete T-Beam Bridges and Load Rating Improvement Through Proxy Finite Element Analysis

UMaine Composites Center Report 20-20-1613

Analysis

```
% Allocate a vector of rating factors
RF = zeros(size(rxn));
% For each girder
for ii = 1:length(rxn)
%     Calculate the effective shear depth (in)
    dv = max([0.9*de(ii),0.72*h(ii),Mn(ii)/(As(ii)*fy)]);
%     Calculate net longitudinal strain
    es = rxn(ii)/Es/As(ii);
%     Calculate beta factor for MCFT
    beta = 4.8/(1+750*es)*51/(39+dv);
%     Calculate theta factor for MCFT
    theta = 29+3500*es;
%     Calculate concrete shear resistance (kip)
    Vc = 0.0316*beta*sqrt(fpc)*bv(ii)*dv;
%     Calculate steel shear resistance (kip)
    Vs = Av(ii)*fy*dv*cotd(theta)/s(ii);
%     Calculate total shear resistance (kip)
    Vn = min([Vs+Vc,0.25*fpc*bv(ii)*dv]);
%     Calculate rating factor
    RF(ii) = (Vn-DL_rxn(ii))/(rxn(ii)*load_factor);
end
```

Published with MATLAB® R2017b